

Geometry of Linear Neural Networks: Equivariance and Invariance under Permutation Groups

Kathlén Kohn^b, Anna-Laura Sattelberger^b, and Vahid Shahverdi^b

Abstract

The set of functions parameterized by a linear fully-connected neural network is a determinantal variety. We investigate the subvariety of functions that are equivariant or invariant under the action of a permutation group. Examples of such group actions are translations or 90° rotations on images. We describe such equivariant or invariant subvarieties as direct products of determinantal varieties, from which we deduce their dimension, degree, Euclidean distance degree, and their singularities. We fully characterize invariance for arbitrary permutation groups, and equivariance for cyclic groups. We draw conclusions for the parameterization and the design of equivariant and invariant linear networks in terms of sparsity and weight-sharing properties. We prove that all invariant linear functions can be parameterized by a single linear autoencoder with a weight-sharing property imposed by the cycle decomposition of the considered permutation. The space of rank-bounded equivariant functions has several irreducible components, so it can *not* be parameterized by a single network—but each irreducible component can. Finally, we show that minimizing the squared-error loss on our invariant or equivariant networks reduces to minimizing the Euclidean distance from determinantal varieties via the Eckart–Young theorem.

Contents

1	Introduction	2
2	Warm-up and preliminaries	4
3	Invariance under permutation groups	16
4	Equivariance under cyclic subgroups of the symmetric group	21
5	Experiments	35
6	Conclusion and outlook	39
	References	40

^b Department of Mathematics, KTH Royal Institute of Technology, 100 44 Stockholm, Sweden
kathlen@kth.se, alsat@kth.se, and vahidsha@kth.se

1 Introduction

Neural networks that are equivariant or invariant under the action of a group attract high interest both in applications and in the theory of machine learning. It is important to thoroughly study their fundamental properties. While invariance is important for classifiers, equivariance typically comes into play in feature extraction tasks. Modding out such symmetries can drastically reduce time and memory needed for the training of neural networks. Taking carbon emissions during the training of models [6] into account, it is important for the role of AI in the climate crisis to encounter the increasing training and hence energy costs. This is also one of the aims that the initiative *Green AI* [16] is thriving for, to which the construction of group equi- or invariant neural networks might contribute.

The present article investigates linear neural networks. An example of them are linear encoder-decoder models: they are families of functions $\{f_\theta\}_{\theta \in \Theta}$, parameterized by a set $\Theta = \mathbb{R}^{n \times r} \times \mathbb{R}^{r \times n}$. For each parameter $\theta \in \Theta$, the function f_θ is a composition of linear maps

$$f_\theta: \mathbb{R}^n \xrightarrow{f_{1,\theta}} \mathbb{R}^r \xrightarrow{f_{2,\theta}} \mathbb{R}^n, \quad (1.1)$$

where $r \leq n$. One commonly visualizes f_θ as in Figure 1.

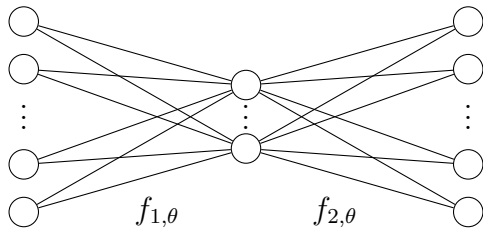


Figure 1: A fully-connected network of depth 2.

If $n = p^2$ is a square number, one can think of the input of the network as a quadratic image with $p \times p$ pixels. If $n = p^3$, the input might be a cubic 3D scenery. In applications, one often aims to learn functions that are equi- or invariant under certain group actions, such as translations, rotations, or reflections.

The function space of a linear fully-connected neural network is a determinantal variety: For natural numbers r, m, n , we write $\mathcal{M}_{r,m \times n}$ for the subvariety of $\mathbb{C}^{m \times n}$ whose points are complex $m \times n$ matrices of rank at most r . In learning tasks, *real* matrices of rank at most r are in use; these are precisely the real-valued points $\mathcal{M}_{r,m \times n}(\mathbb{R})$ of $\mathcal{M}_{r,m \times n}$. Reading the entries of a matrix M as variables, the variety $\mathcal{M}_{r,m \times n}$ is the locus of simultaneous vanishing of all $(r+1) \times (r+1)$ minors of M . For a linear fully-connected neural network with input dimension n , output dimension m , and whose smallest layer has width r , the set of functions parameterized by it is exactly $\mathcal{M}_{r,m \times n}(\mathbb{R})$.

A good understanding of the geometry of the function space of a neural network is not only mathematically interesting per se. It is useful to understand the training process of a network. For instance, it is important for understanding the type of the critical points of the loss function. This behavior typically varies from architecture to architecture. In the case

of linear fully-connected networks, critical points often correspond to matrices of rank even lower than r , i.e., they lie in the singular locus of the determinantal variety $\mathcal{M}_{r,m \times n}(\mathbb{R})$ [17]. Investigating those points is crucial for proving the convergence of such networks to nice minima [15]. The nature of critical points is very different in the case of linear convolutional networks. Here, critical points are almost always smooth points of the function space [12, 13].

Main results. In the present article, we investigate the subvarieties $\mathcal{E}_{r,n \times n}^G \subset \mathcal{M}_{r,n \times n}$ and $\mathcal{I}_{r,m \times n}^G \subset \mathcal{M}_{r,m \times n}$ of linear functions of bounded rank that are equivariant and invariant under the action of a permutation group G , respectively. The group G is a subgroup of the symmetric group \mathcal{S}_n and acts on the input and output space \mathbb{R}^n (or \mathbb{R}^m , respectively) by permuting the entries of the input or output vector. For $m = n$, the subvarieties $\mathcal{E}_{r,n \times n}^G$ and $\mathcal{I}_{r,n \times n}^G$ encode the part of the function space of a linear autoencoder that is equi- or invariant under the action of G , respectively. We provide an algebraic characterization of $\mathcal{I}_{r,m \times n}^G$ for arbitrary permutation groups, and for cyclic subgroups of \mathcal{S}_n in the case of equivariance. Our results allow for implications on the design of equi- and invariant networks.

For invariant autoencoders, we prove a weight-sharing property on the encoder and deduce a rank constraint, i.e., a constraint on the width of the middle layer. We prove that the function space of such a constrained autoencoder is exactly $\mathcal{I}_{r,n \times n}^G$. In other words, linear autoencoders with our weight-sharing property on the encoder precisely parameterize invariant functions.

For equivariance, we show that the space of rank-bounded equivariant functions $\mathcal{E}_{r,n \times n}^G$ typically has several irreducible components. This implies that there is *no* linear neural network that can parameterize the whole space $\mathcal{E}_{r,n \times n}^G$ at once. Every network can parameterize at most one of the components. This raises the natural question: *Which component should one choose when designing a network, and is there one which is “best”?* We count the irreducible components via integer partitions of a specific form, and prove that they are direct products of determinantal varieties. We show that each of them can be parameterized by an autoencoder whose encoder and decoder have the same sparsity and weight-sharing pattern.

We also investigate the squared-error loss for our equi- and invariant autoencoders by relating it to Euclidean distance optimization on their function spaces. More concretely, we provide linear transformations that minimize the squared-error loss by minimizing the Frobenius norm on determinantal varieties which can be done using the Eckart–Young theorem. We point out that this approach cannot generally be applied to arbitrary subvarieties of $\mathcal{M}_{r,m \times n}$; it is a special feature of the varieties $\mathcal{E}_{r,n \times n}^G$ and $\mathcal{I}_{r,m \times n}^G$. To that end, we introduce the *squared-error degree* as an algebraic complexity measure for minimizing the squared-error loss on a real variety, and compare it to the (generic) Euclidean distance degree.

To showcase our results, we train linear autoencoders on the MNIST dataset, comparing architectures with and without imposed equivariance under horizontal shifts.

Since it is a common strategy to build nonlinear equivariant networks from linear equivariant layers, we would like to highlight that our findings cannot only be applied to linear networks, but also to the individual layers of nonlinear networks.

Related work. We here give a petite sample of related references, which is by no means claimed to be exhaustive. An overview of equivariant neural networks is provided in the survey [14]. The study of equivariance has roots in pattern recognition [20]. Group-equivariant convolutional networks were introduced by Cohen and Welling in [4], allowing for applications in image analysis [1]. In [2], transitive group actions are considered. Therein, Bekkers proves that, on the level of feature maps, a linear map is equivariant if and only if it is a group convolution. Isometry- and gauge-equivariant CNNs on Riemannian manifolds were investigated in [19]. This geometric perspective has strong connections to physics.

To the best of our knowledge, our article is the first one to tackle the *algebro-geometric* study of equi- or invariant networks, their function spaces, and squared-error loss minimization on these spaces.

Notation. By \mathcal{F} , we denote the function space, and by Θ the parameter space of a neural network $F: \Theta \rightarrow \mathcal{F}$. For a parameter $\theta \in \Theta$, we denote the function $F(\theta)$ by f_θ . The symbol \mathbb{K} denotes one of the fields $\{\mathbb{R}, \mathbb{C}\}$. For an ideal I in a polynomial ring $\mathbb{K}[x_1, \dots, x_n]$, we denote by $V(I)$ the algebraic variety $V(I) = \{x \in \mathbb{K}^n \mid p(x) = 0 \text{ for all } p \in I\}$. The symbol $\mathcal{M}_{r,m \times n}$ denotes the determinantal variety in $\mathbb{C}^{m \times n}$ whose points are complex $m \times n$ matrices M of rank at most r , and $\mathcal{M}_{r,m \times n}(\mathbb{R})$ its real-valued points, i.e., real matrices M of rank at most r . Its subsets of equi- and invariant subspaces under the action of a group G will be denoted by $\mathcal{E}_{r,m \times n}^G$ and $\mathcal{I}_{r,m \times n}^G$, respectively. If the letter r is dropped in the notation, this means that no rank constraint is imposed on the matrices. For fixed $T \in \text{GL}_n(\mathbb{K})$ and any matrix $M \in \mathcal{M}_{n \times n}(\mathbb{K})$, we write shortly $M^{\sim T} := T^{-1}MT$ for the respective similarity transform. We denote the identity matrix of size n by I_n , and by \mathcal{S}_n the symmetric group on the set $[n] = \{1, \dots, n\}$. For a permutation $\sigma \in \mathcal{S}_n$, $\mathcal{P}(\sigma)$ denotes the partition $\{A_1, \dots, A_k\}$ of the set $[n]$ induced by the decomposition $\sigma = \pi_1 \circ \dots \circ \pi_k$ of σ into pairwise disjoint cycles π_i , where we also count trivial cycles, i.e., cycles of length 1.

Outline. In Section 2, we present motivating examples, basics about squared-error loss minimization, and necessary preliminaries from (non-)linear algebra. In particular, we introduce the notion of *squared-error degree*. Section 3 treats invariance under arbitrary permutation groups. Section 4 characterizes equivariance of linear autoencoders under cyclic subgroups of the symmetric group. To demonstrate our results, we run experiments on the MNIST dataset in Section 5, comparing different architectures. In Section 6, we present which other groups and further generalizations we are planning to tackle in future work.

2 Warm-up and preliminaries

We start with cyclic subgroups G of the symmetric group \mathcal{S}_n , i.e., groups of the form $G = \langle \sigma \rangle$ for some permutation $\sigma \in \mathcal{S}_n$. Such groups G naturally act on the input space \mathbb{R}^n and the output space \mathbb{R}^n of the network (1.1) by permuting the entries of the in- and output vector, respectively, and on linear maps $f: \mathbb{R}^n \rightarrow \mathbb{R}^m$ by permuting the columns of the $m \times n$ matrix representing f .

and let $G = \langle \sigma \rangle$. This is a finite, cyclic subgroup of $O(2)$ which preserves the $p \times p$ shape of the input matrix, which we interpret as a quadratic image with $n = 9$ real pixels a_{ij} . We are interested in those maps that are equivariant under G , i.e., linear maps f for which

$$\sigma \circ f = f \circ \sigma. \quad (2.9)$$

Again, we identify $\mathbb{R}^{3 \times 3} \cong \mathbb{R}^9$ via

$$\begin{pmatrix} a_{11} & a_{12} & a_{13} \\ a_{21} & a_{22} & a_{23} \\ a_{31} & a_{32} & a_{33} \end{pmatrix} \mapsto (a_{11} \ a_{13} \ a_{33} \ a_{31} \ a_{12} \ a_{23} \ a_{32} \ a_{21} \ a_{22})^\top. \quad (2.10)$$

Then $\sigma(A)$ is represented by the vector $(a_{31} \ a_{11} \ a_{13} \ a_{33} \ a_{21} \ a_{12} \ a_{23} \ a_{32} \ a_{22})^\top$. Under this identification, the rotation is the permutation $\sigma = (1 \ 4 \ 3 \ 2)(5 \ 8 \ 7 \ 6) \in \mathcal{S}_9$ and is represented by

$$\left(\begin{array}{cccc|ccc|c} 0 & 0 & 0 & 1 & & & & 0 \\ 1 & 0 & 0 & 0 & & 0 & & 0 \\ 0 & 1 & 0 & 0 & & & & \\ 0 & 0 & 1 & 0 & & & & \\ \hline & & & & 0 & 0 & 0 & 1 \\ & & & & 1 & 0 & 0 & 0 \\ & & & & 0 & 1 & 0 & 0 \\ & & & & 0 & 0 & 1 & 0 \\ \hline & & & & 0 & & & 1 \end{array} \right). \quad (2.11)$$

from Equation (2.3). A map f is equivariant under σ , and hence under G , if and only if its representing matrix M satisfies

$$P_\sigma \cdot M = M \cdot P_\sigma. \quad (2.12)$$

We therefore aim to determine all matrices M that commute with P_σ . Hence, a matrix M is equivariant under σ if and only if M is similar to itself with the permutation matrix of σ as base change. Also condition (2.9) can be expressed as the vanishing of polynomials read from Equation (2.12). Those 81 homogeneous binomials of degree 1 cut out the vector space $\mathcal{E}_{9 \times 9}^\sigma$. We see from (2.11) that the matrices in $\mathcal{E}_{9 \times 9}^\sigma$ must be of the form

$$\left(\begin{array}{cccc|cccc|c} \alpha_1 & \alpha_2 & \alpha_3 & \alpha_4 & \beta_1 & \beta_2 & \beta_3 & \beta_4 & \varepsilon_3 \\ \alpha_4 & \alpha_1 & \alpha_2 & \alpha_3 & \beta_4 & \beta_1 & \beta_2 & \beta_3 & \varepsilon_3 \\ \alpha_3 & \alpha_4 & \alpha_1 & \alpha_2 & \beta_3 & \beta_4 & \beta_1 & \beta_2 & \varepsilon_3 \\ \alpha_2 & \alpha_3 & \alpha_4 & \alpha_1 & \beta_2 & \beta_3 & \beta_4 & \beta_1 & \varepsilon_3 \\ \hline \gamma_1 & \gamma_2 & \gamma_3 & \gamma_4 & \delta_1 & \delta_2 & \delta_3 & \delta_4 & \varepsilon_4 \\ \gamma_4 & \gamma_1 & \gamma_2 & \gamma_3 & \delta_4 & \delta_1 & \delta_2 & \delta_3 & \varepsilon_4 \\ \gamma_3 & \gamma_4 & \gamma_1 & \gamma_2 & \delta_3 & \delta_4 & \delta_1 & \delta_2 & \varepsilon_4 \\ \gamma_2 & \gamma_3 & \gamma_4 & \gamma_1 & \delta_2 & \delta_3 & \delta_4 & \delta_1 & \varepsilon_4 \\ \hline \varepsilon_1 & \varepsilon_1 & \varepsilon_1 & \varepsilon_1 & \varepsilon_2 & \varepsilon_2 & \varepsilon_2 & \varepsilon_2 & \varepsilon_5 \end{array} \right). \quad (2.13)$$

Hence, the dimension of the vector space $\mathcal{E}_{9 \times 9}^\sigma$ is $81 - 60 = 4 \cdot 4 + 5 \cdot 1 = 21$. The matrices in this vector space that lie in the function space of the autoencoder (2.6) form the variety $\mathcal{E}_{3,9 \times 9}^\sigma$, which is obtained as the intersection of \mathcal{E}^σ and $\mathcal{M}_{3,9 \times 9}$, i.e.,

$$\mathcal{E}_{3,9 \times 9}^\sigma = \mathcal{M}_{3,9 \times 9} \cap \mathcal{E}_{9 \times 9}^\sigma. \quad (2.14)$$

In Theorems 4.2 and 4.8, we will see that this variety has 17 irreducible components over \mathbb{C} , and 5 irreducible components over \mathbb{R} . The latter implies that there is *no* linear neural network whose function space equals $\mathcal{E}_{3,9 \times 9}^\sigma$. We will explain in Section 4.3 how one can construct five autoencoders whose function spaces are the five real irreducible components of $\mathcal{E}_{3,9 \times 9}^\sigma$. Note that also the determinant of the matrix (2.13), cutting out $\mathcal{E}_{8,9 \times 9}^\sigma$, is reducible: over \mathbb{R} , it has three factors; one of them factorizes over the complex numbers, resulting in a total of four factors over \mathbb{C} .

2.2 Squared-error loss & Euclidean distance minimization

Consider a linear network whose function space \mathcal{F} is contained in $\mathcal{M}_{m \times n}(\mathbb{R})$. Given training data $\mathcal{D} = \{(x_i, y_i) \mid i = 1, \dots, d\} \subset \mathbb{R}^n \times \mathbb{R}^m$ consisting of input and output pairs (x_i, y_i) , we collect all these in- and output vectors as the columns of matrices $X \in \mathbb{R}^{n \times d}$ and $Y \in \mathbb{R}^{m \times d}$, respectively. The *squared-error loss* with respect to the data matrices X and Y then is

$$\mathcal{M}_{m \times n}(\mathbb{R}) \rightarrow \mathbb{R}, \quad M \mapsto \|MX - Y\|_F^2, \quad (2.15)$$

where $\|\cdot\|_F$ denotes the Frobenius norm. Given sufficiently many training data (more specifically, $d \geq n$) that are sufficiently generic, minimizing the squared-error loss on the function space $\mathcal{F} \subset \mathcal{M}_{m \times n}(\mathbb{R})$ is equivalent to minimizing a weighted Euclidean distance on \mathcal{F} :

Lemma 2.3. *If $\text{rank}(XX^\top) = n$, then*

$$\arg \min_{M \in \mathcal{F}} \|MX - Y\|_F^2 = \arg \min_{M \in \mathcal{F}} \|M - U\|_{XX^\top}^2, \quad \text{where } U := YX^\top (XX^\top)^{-1}. \quad (2.16)$$

In the lemma, $\|\cdot\|_{XX^\top}$ denotes the norm induced by the inner product given by the positive definite matrix XX^\top , which is defined as

$$\langle A, B \rangle_{XX^\top} := \langle A(XX^\top)^{1/2}, B(XX^\top)^{1/2} \rangle_F. \quad (2.17)$$

Proof of Lemma 2.3. We start by observing that

$$\langle M, U \rangle_{XX^\top} = \text{tr}(MXX^\top U^\top) = \text{tr}(MXY^\top) = \langle MX, Y \rangle_F, \quad (2.18)$$

from which we obtain that

$$\begin{aligned} \|MX - Y\|_F^2 &= \langle MX, MX \rangle_F - 2\langle MX, Y \rangle_F + \langle Y, Y \rangle_F \\ &= \langle M, M \rangle_{XX^\top} - 2\langle M, U \rangle_{XX^\top} + \langle Y, Y \rangle_F \\ &= \|M - U\|_{XX^\top}^2 + (\langle Y, Y \rangle_F - \langle U, U \rangle_{XX^\top}). \end{aligned} \quad (2.19)$$

The last term, in parentheses, is constant in the sense that it does not depend on M , but only on the data matrices X and Y . This proves the assertion. \square

Let us first consider the case where XX^\top is (close to) a multiple of the identity matrix. For instance, when x_1, \dots, x_d are samples drawn from a multivariate normal distribution $\mathcal{N}(0, \sigma I_n)$, then the matrix XX^\top converges to $\sigma^2 I_n$ as the number of samples d tends to infinity. In that case, (2.16) is the problem of finding a point in the function space \mathcal{F} that is closest to the point U with respect to the standard Euclidean (i.e., Frobenius) distance. We will see in Proposition 3.8 and Section 4.2 that, when \mathcal{F} is either $\mathcal{I}_{r,m \times n}^G$ or one of the real irreducible components of $\mathcal{E}_{r,m \times n}^\sigma$, the minimum in (2.16) can be easily found using singular value decompositions and the Eckart–Young theorem, which we recall now. Given a matrix $U \in \mathcal{M}_{m \times n}(\mathbb{R})$, we write $U = V_1 \cdot \text{diag}(\sigma_1, \sigma_2, \dots, \sigma_{\min(m,n)}) \cdot V_2$ for its singular value decomposition, where $\sigma_1 \geq \sigma_2 \geq \dots \geq \sigma_{\min(m,n)}$ and V_1 and V_2 are orthogonal matrices.

Theorem 2.4 (Eckart–Young). *A solution to $\arg \min_{M \in \mathcal{M}_{r,m \times n}(\mathbb{R})} \|M - U\|_F^2$ is*

$$U^* = V_1 \cdot \text{diag}(\sigma_1, \dots, \sigma_r, 0, \dots, 0) \cdot V_2. \quad (2.20)$$

If U has pairwise distinct singular values, then U^ is the unique local minimum.*

In the case when XX^\top is not a multiple of the identity, but another matrix of full rank, the optimization problem (2.16) can be more complicated.

Example 2.5. When $\mathcal{F} = \mathcal{M}_{r,m \times n}(\mathbb{R})$ is the function space of a fully-connected linear network, then the problem (2.16) is actually always equivalent to distance minimization under the standard Euclidean norm. More concretely, since the left-multiplication by the positive definite matrix $(XX^\top)^{1/2}$ is an automorphism on \mathcal{F} , we have

$$\left(\arg \min_{M \in \mathcal{M}_{r,m \times n}(\mathbb{R})} \|M - U\|_{XX^\top}^2 \right) \cdot (XX^\top)^{1/2} = \arg \min_{M \in \mathcal{M}_{r,m \times n}(\mathbb{R})} \|M - U(XX^\top)^{1/2}\|_F^2. \quad (2.21)$$

Hence, we can solve (2.16) by solving the right-hand side of (2.21) by Eckart–Young. \diamond

However, when the multiplication by positive definite matrices does not leave the function space \mathcal{F} invariant, then the argument presented in Example 2.5 does not apply and the optimization problem in (2.16) can in general not be solved using Eckart–Young. In such a situation, in order to find a global minimum of (2.16), one might have to compute all complex critical points of the optimization problem, then discard the non-real ones, and finally determine the minimum among the remaining real critical points. The benefit of working over the complex numbers is that the number of complex critical points is the same for almost all data matrices X and Y whenever \mathcal{F} is Zariski closed. This number measures the algebraic complexity of the minimization problem (2.16), and we refer to it as the *squared-error degree* of the algebraic variety \mathcal{F} .

Definition 2.6. Let \mathcal{F} be a subvariety of $\mathcal{M}_{m \times n}(\mathbb{R})$, and $X \in \mathbb{R}^{n \times n}$ and $Y \in \mathbb{R}^{m \times n}$ generic matrices. The *squared-error degree* of \mathcal{F} is the number of complex critical points of the squared-error loss (2.15) restricted to \mathcal{F} . We denote it by $\text{SEdegree}(\mathcal{F})$.

If X is of the special form such that XX^\top is a multiple of the identity matrix, then the squared-error degree specializes to the *Euclidean distance degree* of \mathcal{F} , introduced in [8]. We denote it by $\text{EDdegree}(\mathcal{F})$. By Example 2.5, we see that

$$\text{SEdegree}(\mathcal{M}_{r,m \times n}(\mathbb{R})) = \text{EDdegree}(\mathcal{M}_{r,m \times n}(\mathbb{R})), \quad (2.22)$$

but in general, the squared-error degree is not equal to the Euclidean distance degree.

Example 2.7. Let \mathcal{F} be the space of 2×2 Hankel matrices $\begin{pmatrix} a & b \\ b & c \end{pmatrix}$ of rank at most one. A computation in Macaulay2 [10] shows that $\text{EDdegree}(\mathcal{F}) = 2$ and $\text{SEdegree}(\mathcal{F}) = 4$. \diamond

Remark 2.8. There is also a notion of *generic* Euclidean distance degree of a subvariety $\mathcal{F} \subset \mathcal{M}_{m \times n}(\mathbb{R})$, see [3, Chapter 2]. It is the number of complex critical points of the map

$$\mathcal{F} \longrightarrow \mathbb{R}, \quad M \mapsto \sum_{i=1}^m \sum_{j=1}^n \lambda_{ij} \cdot (m_{ij} - u_{ij})^2, \quad (2.23)$$

where $U = (u_{ij})_{i,j}$, $\Lambda = (\lambda_{ij})_{i,j} \in \mathcal{M}_{m \times n}(\mathbb{R})$ are generic matrices. Squared-error loss minimization in (2.16) is a special case of (2.23), where the positive definite matrix XX^\top determines the weight matrix Λ . Hence, the following relations hold:

$$\text{EDdegree}(\mathcal{F}) \leq \text{SEdegree}(\mathcal{F}) \leq \text{genericEDdegree}(\mathcal{F}). \quad (2.24)$$

Both inequalities can be equalities or strict inequalities. In Example 2.7, the three optimization degrees in (2.24) are $2 < 4 = 4$. For $\mathcal{F} = \mathcal{M}_{1,2 \times 2}(\mathbb{R})$, they are $2 = 2 < 6$. \diamond

For the case that \mathcal{F} is either $\mathcal{I}_{r,m \times n}^G$ or one of the real irreducible components of $\mathcal{E}_{r,m \times n}^\sigma$, we will show in Proposition 3.8 and Section 4.2 that the squared-error loss minimization in (2.16) can be reduced to standard Euclidean distance minimization and solved explicitly using Eckart–Young, which in particular implies that $\text{SEdegree}(\mathcal{F}) = \text{EDdegree}(\mathcal{F})$. For the irreducible components of $\mathcal{E}_{r,m \times n}^\sigma$, we will make use of the following crucial property of squared-error minimization.

Lemma 2.9. *Let $\mathcal{F}_1 \subset \mathcal{M}_{m_1 \times n_1}(\mathbb{R})$ and $\mathcal{F}_2 \subset \mathcal{M}_{m_2 \times n_2}(\mathbb{R})$ be subvarieties. Consider their direct product $\mathcal{F} := \mathcal{F}_1 \times \mathcal{F}_2$. I.e., the elements of \mathcal{F} are block diagonal matrices $M_1 \oplus M_2$ with blocks $M_i \in \mathcal{F}_i$. For all matrices $X \in \mathbb{R}^{(n_1+n_2) \times d}$ and $Y \in \mathbb{R}^{(m_1+m_2) \times d}$ with $\text{rank}(XX^\top) = n_1 + n_2$, every minimizer M of the squared-error loss minimization (2.16) is of the form $M = M_1 \oplus M_2$, where M_i is a minimizer of a squared-error loss minimization on \mathcal{F}_i .*

Proof. The minimization problem we need to solve is

$$\arg \min_{M=M_1 \oplus M_2 \in \mathcal{F}_1 \times \mathcal{F}_2} \|M - U\|_{XX^\top}^2 = \arg \min_{M=M_1 \oplus M_2 \in \mathcal{F}_1 \times \mathcal{F}_2} \|(M - U)X\|_F^2. \quad (2.25)$$

After projecting U orthogonally onto the linear space of block diagonal matrices (with respect to the inner product $\langle \cdot, \cdot \rangle_{XX^\top}$), we may assume that $U = U_1 \oplus U_2$ has the same block diagonal form as M . Now, we let X_1 be the matrix that consists of the first n_1 rows of X , and let X_2

consist of the remaining n_2 rows, i.e., $X = \begin{pmatrix} X_1 \\ X_2 \end{pmatrix}$. Then, $(M - U)X = \begin{pmatrix} (M_1 - U_1)X_1 \\ (M_2 - U_2)X_2 \end{pmatrix}$, which shows that (2.25) is

$$\arg \min_{M_1 \oplus M_2 \in \mathcal{F}_1 \times \mathcal{F}_2} \sum_{i=1}^2 \|(M_i - U_i)X_i\|_F^2 = \arg \min_{M_1 \in \mathcal{F}_1} \|M_1 - U_1\|_{X_1 X_1^\top}^2 \oplus \arg \min_{M_2 \in \mathcal{F}_2} \|M_2 - U_2\|_{X_2 X_2^\top}^2.$$

By Lemma 2.3, the last two minimization problems are squared-error loss minimizations on the individual factors \mathcal{F}_i , since $\text{rank}(X_i X_i^\top) = n_i$. \square

We point out that Euclidean distance minimization on a space of functions is of interest for learning besides its relation to the squared-error loss. For example, consider the scenario where one has learned a function f that is not equivariant under some given group action, but reasonably close to the space of equivariant function. For instance, f could be obtained by training some neural network with a regularized loss that favors functions that are almost equivariant. Then, one can try to turn f into an equivariant function by finding the closest point on the space of equivariant functions to f . For a linear function f represented by a matrix U , that would mean to find a matrix $M \in \mathcal{E}_{r, m \times n}^\sigma$ that minimizes $\|M - U\|_F^2$.

2.3 Algebraic geometry of similarity transforms

For natural numbers m, n and $r \leq \min(m, n)$, the variety $\mathcal{M}_{r, m \times n}$ of $m \times n$ matrices of rank at most r has dimension

$$\dim(\mathcal{M}_{r, m \times n}) = r \cdot (m + n - r), \quad (2.26)$$

cf. [11, Proposition 12.2]. We remind our readers that the dimension of an affine variety means the Krull dimension of its coordinate ring.

Remark 2.10 (Real vs. complex). Since all the coefficients of the contributing polynomials are real, the real variety of real-valued points $\mathcal{M}_{r, m \times n}(\mathbb{R}) = \mathcal{M}_{r, m \times n}(\mathbb{C}) \cap \mathbb{R}^{m \times n}$ of $\mathcal{M}_{r, m \times n}$ has the same dimension as the complex variety $\mathcal{M}_{r, m \times n}$. The points of $\mathcal{M}_{r, m \times n}(\mathbb{R})$ are real $m \times n$ matrices of rank at most r . \diamond

As was pointed out in [11, Example 19.10], it is proven in [9, Example 14.4.11] that the degree of $\mathcal{M}_{r, m \times n}$ is

$$\deg(\mathcal{M}_{r, m \times n}) = \prod_{i=0}^{n-r-1} \frac{(m+i)! \cdot i!}{(r+i)! \cdot (m-r+i)!}. \quad (2.27)$$

Fact 2.11. *Let $0 < r < n$. A matrix $M \in \mathcal{M}_{r, m \times n}$ is a singular point of $\mathcal{M}_{r, m \times n}$ if and only if its rank is strictly smaller than r , i.e., $\text{Sing}(\mathcal{M}_{r, m \times n}) = \mathcal{M}_{r-1, m \times n}$.* \square

The Eckart–Young theorem can be extended to also list all critical points of minimizing the distance from $\mathcal{M}_{r, m \times n}(\mathbb{R})$ to a given matrix U . In fact, every critical point is real and is obtained from a singular value decomposition of U by setting $\min(m, n) - r$ singular values

to zero, similarly as in Theorem 2.4, see [8, Example 2.3]. Hence, the Euclidean distance degree of the determinantal variety $\mathcal{M}_{r,m \times n}(\mathbb{R})$ is $\binom{\min(m,n)}{r}$. By (2.22), this number is also the squared-error degree, i.e.,

$$\text{SEdegree}(\mathcal{M}_{r,m \times n}(\mathbb{R})) = \text{EDdegree}(\mathcal{M}_{r,m \times n}(\mathbb{R})) = \binom{\min(m,n)}{r}. \quad (2.28)$$

In our investigations, we will commonly perform base changes of the matrices in $\mathcal{M}_{m \times n}$. For a subvariety $\mathcal{X} \subset \mathcal{M}_{m \times n}$ and any $T \in \text{GL}_n$, we denote by \mathcal{X}^T the image of \mathcal{X} under the linear isomorphism

$$\cdot T: \mathcal{M}_{m \times n} \longrightarrow \mathcal{M}_{m \times n}, \quad M \mapsto MT. \quad (2.29)$$

Lemma 2.12. *Let $\mathcal{X} \subset \mathcal{M}_{m \times n}$ be a subvariety and let $T \in \text{GL}_n$. Then, $\dim(\mathcal{X}^T) = \dim \mathcal{X}$, $\deg(\mathcal{X}^T) = \deg \mathcal{X}$, $\text{SEdegree}(\mathcal{X}^T) = \text{SEdegree}(\mathcal{X})$, $\text{Sing}(\mathcal{X}^T) = \text{Sing}(\mathcal{X})^T$, and $(\mathcal{X}^T) \cap \mathcal{M}_{r,m \times n} = (\mathcal{X} \cap \mathcal{M}_{r,m \times n})^T$ for any $r \leq \min(m, n)$.*

Proof. Since (2.29) is a linear isomorphism, it preserves the dimension and the degree, and maps regular points to regular points. Due to the genericity of X in Definition 2.6, the squared-error degree is not affected by that isomorphism. For the last assertion, we observe that every matrix $M \in \mathcal{M}_{m \times n}$ satisfies that $\text{rank}(MT) = \text{rank}(M)$, since T has full rank. \square

We point out that the Euclidean distance degree (short, ED degree) is in general not preserved by the isomorphism (2.29) as the following example demonstrates.

Example 2.13. Let $m = 1$ and $n = 3$. Consider the circle $\mathcal{X} \subset \mathcal{M}_{1 \times 3}(\mathbb{C})$ defined by the equation $M_{1,1}^2 + M_{1,2}^2 - M_{1,3}^2 = 0$. The ED degree of $\mathcal{X}(\mathbb{R})$ in the standard Euclidean distance

$$d(0, M) := \|M\|^2 = \text{tr}(MM^\top) = M_{1,1}^2 + M_{1,2}^2 + M_{1,3}^2 \quad (2.30)$$

is equal to 2. Throughout this article, we often consider permutation matrices and diagonalize them. For instance to diagonalize the permutation matrix $P := \begin{pmatrix} 0 & 0 & 1 \\ 1 & 0 & 0 \\ 0 & 1 & 0 \end{pmatrix}$, we use the symmetric Vandermonde matrix

$$T := V(1, \zeta_3, \zeta_3^2) = \begin{pmatrix} 1 & 1 & 1 \\ 1 & \zeta_3 & \zeta_3^2 \\ 1 & \zeta_3^2 & \zeta_3 \end{pmatrix},$$

where ζ_3 is any primitive third root of unity. In fact, we obtain $T^{-1}PT = \text{diag}(1, \zeta_3^2, \zeta_3)$. The ED degree of $\mathcal{X}^T(\mathbb{R})$ is not equal to 2 anymore. In fact, the ED degree of \mathcal{X}^T counts the critical points of the function $d(0, MT - U)$ over all $M \in \mathcal{X}(\mathbb{R})$ for fixed, generic U . Since U is generic, we can replace it by UT . Hence, the ED degree of \mathcal{X}^T under the standard Euclidean distance (2.30) is equal to the ED degree of \mathcal{X} under the modified Euclidean distance

$$d_T(0, M) := d(0, MT) = 3 \cdot (M_{1,1}^2 + 2M_{1,2}M_{1,3}).$$

A computation in Macaulay2 shows that the ED degree of $\mathcal{X}(\mathbb{R})$ under d_T is 4. \diamond

However, the ED degree does keep unchanged under the multiplication by an orthogonal matrix by the right.

Lemma 2.14. *Consider a variety $\mathcal{X} \subset \mathcal{M}_{m \times n}(\mathbb{R})$ and let $T \in O(n)$ be an orthogonal matrix. Then $\text{EDdegree}(\mathcal{X}) = \text{EDdegree}(\mathcal{X}^T)$.*

Proof. Let $U \in \mathcal{M}_{m \times n}(\mathbb{R})$ be generic and T an orthogonal $n \times n$ matrix. Then

$$\begin{aligned} \min_{X \in \mathcal{X}} \|XT - UT\|^2 &= \min_{X \in \mathcal{X}} (\text{tr}((X - U)T \cdot ((X - U)T)^\top)) \\ &= \min_{X \in \mathcal{X}} (\text{tr}((X - U) \cdot (X - U)^\top)) \\ &= \min_{X \in \mathcal{X}} \|X - U\|^2, \end{aligned} \tag{2.31}$$

resulting in the same number of critical points for minimizing over \mathcal{X} and \mathcal{X}^T , resp. \square

Depending on whether we study invariance or equivariance, we perform base changes on only one side of the matrices, or on both sides. For the latter, we write $M^{\sim T} := T^{-1}MT$ for given matrices $M \in \mathcal{M}_{n \times n}$ and $T \in \text{GL}_n$.

Lemma 2.15. *Consider the matrices $M \in \mathcal{M}_{m \times m}$, $P \in \mathcal{M}_{n \times n}$, and $T \in \text{GL}_n$. Then, $MP = M$ if and only if $M^T P^{\sim T} = M^T$. In the case that $m = n$, we moreover have that $MP = PM$ if and only if $M^{\sim T} P^{\sim T} = P^{\sim T} M^{\sim T}$. \square*

In our investigations, we will make use of presentations of permutation matrices P in different bases. The strategy is as follows. Step 1 consists in decomposing a permutation $\sigma \in \mathcal{S}_n$ into disjoint cycles π_1, \dots, π_k of lengths ℓ_1, \dots, ℓ_k ; this brings the permutation matrix P_σ of σ into block diagonal form, where each diagonal block is a circulant matrix. The second step is to diagonalize those circulant matrices of sizes ℓ_1, \dots, ℓ_k . Step 3 is optional and groups the columns corresponding to the same eigenvalue.

Procedure 2.16.

Step 0. Represent σ by the permutation matrix $P_\sigma \in \mathcal{M}_{n \times n}(\{0, 1\})$ with respect to the standard basis of \mathbb{R}^n , i.e., the j -th row of P_σ is the transpose of the $\sigma(j)$ -th standard unit vector of \mathbb{R}^n .

Step 1. Determine a permutation matrix $T_1 \in \mathcal{M}_{n \times n}(\{0, 1\})$ such that $P_\sigma^{\sim T_1} = T_1^{-1}P_\sigma T_1$ is block diagonal whose blocks are circulant matrices C_1, \dots, C_k of the form

$$C_i = \begin{pmatrix} 0 & & & 1 \\ 1 & 0 & & \\ & 1 & \ddots & \\ & & \ddots & \\ & & & 1 & 0 \end{pmatrix} \in \mathcal{M}_{\ell_i \times \ell_i}(\{0, 1\}). \tag{2.32}$$

Each $C_i \in \mathcal{M}_{\ell_i \times \ell_i}(\{0, 1\})$ has ℓ_i -th roots of unity as eigenvalues, namely $\zeta_{\ell_i}^j$, where $j = 0, \dots, \ell_i - 1$, and ζ_n denotes the primitive root of unity $e^{2\pi i/n}$. Depending on

the lengths ℓ_i of the cycles, some of C_i 's might share common eigenvalues. Collect the eigenvalues of all the C_i 's in a set $\{\lambda_1, \lambda_2, \dots, \lambda_s\}$ together with their multiplicities b_1, b_2, \dots, b_s . Note that one of the λ_i 's is equal to 1 and for this \hat{i} , $b_{\hat{i}} = k$.

Step 2. Diagonalize each matrix C_i from (2.32) via a matrix in $\text{GL}_n(\mathbb{C})$; this can be obtained via Vandermonde matrices $V(1, \zeta_{\ell_i}, \dots, \zeta_{\ell_i}^{\ell_i-1})$ as in Example 2.13. The following block diagonal matrix then diagonalizes the block circulant diagonal matrix $P_\sigma^{\sim T_1}$ from Step 1:

$$T_2 = \begin{pmatrix} V(1, \zeta_{\ell_1}, \dots, \zeta_{\ell_1}^{\ell_1-1}) & & & & \\ & \ddots & & & \\ & & \ddots & & \\ & & & \ddots & \\ & & & & V(1, \zeta_{\ell_k}, \dots, \zeta_{\ell_k}^{\ell_k-1}) \end{pmatrix}. \quad (2.33)$$

Step 3. Group identical eigenvalues: determine $T_3 \in \text{GL}_n(\{0, 1\})$ such that the matrix from Step 2 is block diagonal with blocks of the form $\lambda_i I_{b_i}$, i.e., determine T_3 such that

$$T_3^{-1} \cdot (P_\sigma^{\sim T_1})^{\sim T_2} \cdot T_3 = \begin{pmatrix} \lambda_1 I_{b_1} & & & & \\ & \lambda_2 I_{b_2} & & & \\ & & \ddots & & \\ & & & \ddots & \\ & & & & \lambda_s I_{b_s} \end{pmatrix}. \quad (2.34)$$

We demonstrate Steps 0–2 of Procedure 2.16 at an example.

Example 2.17. Consider the permutation $\sigma = \begin{pmatrix} 1 & 2 & 3 & 4 & 5 \\ 3 & 5 & 4 & 1 & 2 \end{pmatrix} \in \mathcal{S}_5$. Then

$$P_\sigma = \begin{pmatrix} 0 & 0 & 1 & 0 & 0 \\ 0 & 0 & 0 & 0 & 1 \\ 0 & 0 & 0 & 1 & 0 \\ 1 & 0 & 0 & 0 & 0 \\ 0 & 1 & 0 & 0 & 0 \end{pmatrix} \xrightarrow{\sim T_1} \left(\begin{array}{ccc|cc} 0 & 0 & 1 & & \\ 1 & 0 & 0 & 0 & \\ 0 & 1 & 0 & & \\ \hline & & & 0 & 1 \\ 0 & & & 1 & 0 \end{array} \right) \xrightarrow{\sim T_2} \begin{pmatrix} 1 & & & & \\ & \zeta_3^2 & & & \\ & & \zeta_3 & & \\ & & & 1 & \\ & & & & -1 \end{pmatrix}$$

with

$$T_1 = \begin{pmatrix} 0 & 0 & 1 & 0 & 0 \\ 0 & 0 & 0 & 1 & 0 \\ 0 & 1 & 0 & 0 & 0 \\ 1 & 0 & 0 & 0 & 0 \\ 0 & 0 & 0 & 0 & 1 \end{pmatrix} \in \mathcal{M}_{5 \times 5}(\{0, 1\}) \quad \text{and} \quad T_2 = \left(\begin{array}{ccc|cc} 1 & 1 & 1 & & \\ 1 & \zeta_3 & \zeta_3^2 & 0 & \\ 1 & \zeta_3^2 & \zeta_3 & & \\ \hline & & & 1 & 1 \\ 0 & & & 1 & -1 \end{array} \right) \in \text{GL}_5(\mathbb{C}),$$

where ζ_3 denotes the primitive 3rd root of unity $e^{2\pi i/3}$. \diamond

Procedure 2.16 requires complex base change matrices T_2 . We will present a real version of this procedure in Section 4.1.2. Both the complex and the real procedure turn a permutation matrix P_σ into a block diagonal matrix P such that no two distinct blocks have eigenvalues in common. We can then easily determine the set of matrices that commute with P , and we denote this vector space by $C(P)$.

Lemma 2.18. *Let $P = [P_{i,j}] = \bigoplus_{i=1}^n P_{i,i}$ be a block diagonal matrix, where each block $P_{i,i}$ is square and such that sets of eigenvalues of the blocks are pairwise disjoint. Then the commutator $C(P)$ of P consists precisely of those block matrices $M = [M_{i,j}] = \bigoplus_{i=1}^n M_{i,i}$ for which each $M_{i,i}$ commutes with $P_{i,i}$.*

In the lemma, M is assumed to be chopped into blocks of the same size pattern as P .

Proof. Consider the matrix $M = [M_{i,j}]$ as a block-matrix, where each block $M_{i,j}$ has the same size as the corresponding block $P_{i,j}$ in the block diagonal matrix P . Our objective is to establish that if M commutes with P , i.e., $MP = PM$, then all off-diagonal blocks $M_{i,j}$ are zero. From the condition $MP = PM$, it follows that for all i and j :

$$M_{i,j} \cdot P_{j,j} = P_{i,i} \cdot M_{i,j}. \quad (2.35)$$

Hence $M_{i,j}P_{j,j}^2 = P_{i,i}M_{i,j}P_{j,j} = P_{i,i}^2M_{i,j}$ by iterating (2.35). Consequently, for any univariate polynomial p , we have

$$M_{i,j} \cdot p(P_{j,j}) = p(P_{i,i}) \cdot M_{i,j}. \quad (2.36)$$

Let p be the characteristic polynomial of $P_{j,j}$. Thus, we have $p(P_{j,j}) = 0$. Writing $p = \prod_k (x - \lambda_k)$, where the λ_k are the eigenvalues of $P_{j,j}$, we see that $p(P_{i,i}) = \prod_k (P_{i,i} - \lambda_k I)$, for $i \neq j$, is invertible, since $P_{i,i}$ and $P_{j,j}$ do not have any eigenvalue in common. Consequently, we deduce from (2.36) that $M_{i,j}$ is the zero matrix. We conclude that M commutes with P if and only if $M_{i,i}$ commutes with $P_{i,i}$ for all $i = 1, \dots, n$. \square

In the subsequent lemma, we determine the dimension of the eigenspaces of P_σ . We are going to leverage this information to compute the dimension of the commutator $C(P_\sigma)$.

Lemma 2.19. *Let P_σ be a permutation matrix of size n with disjoint cycles, whose associated cyclic matrices C_j are square of size ℓ_j . Then the dimension of the eigenspace of P_σ corresponding to an eigenvalue of the form $e^{2\pi i/l}$ is*

$$d_l := \#\{j \text{ such that } l|\ell_j\}. \quad (2.37)$$

In particular, $\dim_{\mathbb{C}}(C(P_\sigma)) = \sum_l \varphi(l) \cdot d_l^2$. Here, φ denotes Euler's φ -function, whose value $\varphi(l)$ is the order of the unit group of $\mathbb{Z}/l\mathbb{Z}$.

Proof. We begin by observing that the eigenvalues of the matrix C_j are the ℓ_j -th roots of unity, of multiplicity one each. Consequently, $e^{2\pi i/l}$ is an eigenvalue of C_j if and only if l divides ℓ_j . Hence, d_l is the number of j for which l divides ℓ_j . Additionally, we find that also the eigenspace corresponding to the eigenvalue $e^{2\pi im/l}$, where $\gcd(m, l) = 1$, has dimension d_l . Over the complex numbers, P_σ is similar to the diagonal matrix $D_\sigma = [D_l^{(m)}]$, where $D_l^{(m)} = e^{2\pi im/l} I_{d_l}$ and (l, m) runs over the set $\{(l, m) \mid m \leq l, \gcd(m, l) = 1\}$ of cardinality $\varphi(l)$. Employing Lemma 2.18, we establish that the commutator $C(D_\sigma)$ consists of arbitrary block diagonal matrices with claimed size of the blocks. Thus, we deduce from Lemma 2.15 that $\dim_{\mathbb{C}}(C(P_\sigma)) = \sum_l \varphi(l) \cdot d_l^2$. \square

3.1 Reduction to cyclic groups

We denote the columns of a matrix $M \in \mathcal{M}_{m \times n}$ by M_1, M_2, \dots, M_n . For a decomposition $\sigma = \pi_1 \circ \dots \circ \pi_k \in \mathcal{S}_n$ into disjoint cycles, we denote by $\mathcal{P}(\sigma) = \{A_1, \dots, A_k\}$ its induced partition of the set $[n]$. The $A_i \subset [n]$ fulfill $\cup_{i=1}^k A_i = [n]$ and $A_i \cap A_j = \emptyset$ whenever $i \neq j$.

Example 3.1. Let $\sigma = (134)(25) \in \mathcal{S}_5$. Its induced partition of $[5] = \{1, 2, 3, 4, 5\}$ is $\mathcal{P}(\sigma) = \{\{1, 3, 4\}, \{2, 5\}\}$. Note that different permutations might induce the same partition: the permutation $\eta = (143)(25) \neq \sigma$ gives rise to the partition $\mathcal{P}(\eta) = \mathcal{P}(\sigma)$ of the set $[5]$. \diamond

Lemma 3.2. *Let $\sigma \in \mathcal{S}_n$ and consider its decomposition $\sigma = \pi_1 \circ \dots \circ \pi_k$ into k disjoint cycles π_1, \dots, π_k . Then*

$$\mathcal{I}_{m \times n}^\sigma = \{M \in \mathcal{M}_{m \times n} \mid \forall A \in \mathcal{P}(\sigma) \forall i, j \in A : M_i = M_j\} \cong \mathcal{M}_{m \times k}. \quad (3.2)$$

Proof. Consider the partition $\mathcal{P}(\sigma) = \{A_1, \dots, A_k\}$ of $[n]$ induced by the decomposition $\sigma = \pi_1 \circ \dots \circ \pi_k$. Assuming invariance of M under σ , each cycle π_i of σ forces some of the columns of M to coincide, namely the columns indexed by $A_i \subset [n]$. For each $A_i \in \mathcal{P}(\sigma)$, we need to remember only one column M_{A_i} of M . For each i , $\text{length}(\pi_i)$ many identical copies of M_{A_i} are listed as columns in M . Deleting all columns except the M_{A_i} gives a linear isomorphism $\mathcal{I}_{m \times n}^\sigma \cong \mathcal{M}_{m \times k}$. \square

Thus, invariance under a permutation σ depends only on the partition $\mathcal{P}(\sigma)$. We also see that any invariant matrix can have at most k pairwise distinct columns:

Corollary 3.3. *If a linear function $f: \mathbb{R}^n \rightarrow \mathbb{R}^m$ is invariant under $\sigma \in \mathcal{S}_n$, then its rank is at most k , the number of disjoint cycles into which σ decomposes.* \square

Invariance under a permutation group G with arbitrarily many generators can be reduced to invariance under cyclic groups, which we make precise in the following proposition.

Lemma 3.4. *Let $G = \langle \sigma_1, \sigma_2, \dots, \sigma_g \rangle \leq \mathcal{S}_n$ be a permutation group. There exists $\sigma \in \mathcal{S}_n$ such that $\mathcal{I}_{m \times n}^G = \mathcal{I}_{m \times n}^\sigma$. In fact, this equality holds for any $\sigma \in \mathcal{S}_n$ whose induced partition $\mathcal{P}(\sigma)$ is the finest common coarsening of the partitions $\mathcal{P}(\sigma_1), \mathcal{P}(\sigma_2), \dots, \mathcal{P}(\sigma_g)$.*

Proof. Decompose each σ_i into pairwise disjoint cycles $\pi_{i,1} \circ \dots \circ \pi_{i,k_i}$. Invariance of a matrix M under σ_i forces some of the columns of M to coincide and depends only on the partition $\mathcal{P}(\sigma_i)$ of $[n]$. Any additional σ_j , $j \neq i$, forces further columns of M to coincide. Invariance of M under G is hence described by the finest common coarsening of $\mathcal{P}(\sigma_1), \dots, \mathcal{P}(\sigma_g)$. \square

3.2 Characterization of $\mathcal{I}_{r, m \times n}^G$

By Lemma 3.4, it is sufficient to consider cyclic groups. By omitting repeated columns as in Lemma 3.2, we see that $\mathcal{I}_{r, m \times n}^G$ is linearly isomorphic to $\mathcal{M}_{\min(r, k), m \times k}$.

Proposition 3.5. *Let $G = \langle \sigma \rangle \leq \mathcal{S}_n$ be cyclic, and $\sigma = \pi_1 \circ \dots \circ \pi_k$ a decomposition into pairwise disjoint cycles π_i . The variety $\mathcal{I}_{r, m \times n}^G$ is isomorphic to the determinantal variety $\mathcal{M}_{\min(r, k), m \times k}$ via a linear morphism that deletes repeated columns:*

$$\psi_{\mathcal{P}(\sigma)}: \mathcal{I}_{r, m \times n}^G \rightarrow \mathcal{M}_{\min(r, k), m \times k}. \quad (3.3)$$

Proof. For each $A_i \in \mathcal{P}(\sigma)$, $\Psi_{\mathcal{P}(\sigma)}$ remembers the column M_{A_i} of M . Intersecting with $\mathcal{M}_{r,m \times n}$ imposes linear dependencies on the columns of M . This mapping rule is linear in the entries of M . To invert $\psi_{\mathcal{P}(\sigma)}$, one needs to remember $\mathcal{P}(\sigma)$ as datum. \square

Example 3.6 ($m = 2, n = 5, r = 1$). Let $\sigma = (134)(25) \in \mathcal{S}_5$ and hence $k = 2$. Any invariant matrix $M \in \mathcal{M}_{2 \times 5}(\mathbb{R})$ is of the form $\begin{pmatrix} \alpha & \gamma & \alpha & \alpha & \gamma \\ \beta & \delta & \beta & \beta & \delta \end{pmatrix}$ for some $\alpha, \beta, \gamma, \delta \in \mathbb{R}$. The rank constraint $r = 1$ imposes that $(\gamma, \delta) = \lambda \cdot (\alpha, \beta)^\top$ for some $\lambda \in \mathbb{R}$, where we assume w.l.o.g. that $(\alpha, \beta) \neq (0, 0)$ in the case of rank one. The morphism (3.3) hence is

$$\psi_{\mathcal{P}(\sigma)}: \begin{pmatrix} \alpha & \lambda\alpha & \alpha & \alpha & \lambda\alpha \\ \beta & \lambda\beta & \beta & \beta & \lambda\beta \end{pmatrix} \mapsto \begin{pmatrix} \alpha & \lambda\alpha \\ \beta & \lambda\beta \end{pmatrix}. \quad (3.4)$$

To invert the morphism $\psi_{\mathcal{P}(\sigma)}$, one reads from $\mathcal{P}(\sigma)$ how to copy and paste the columns $(\alpha, \beta)^\top$ and $(\lambda\alpha, \lambda\beta)^\top$ to recover the 2×5 matrix one started with. \diamond

Corollary 3.7. *In the setup of Proposition 3.5, one has*

$$\begin{aligned} \dim(\mathcal{I}_{r,m \times n}^\sigma) &= \min(r, k) \cdot (m + k - \min(r, k)), \\ \deg(\mathcal{I}_{r,m \times n}^\sigma) &= \prod_{i=0}^{k-\min(r,k)-1} \frac{(m+i)! \cdot i!}{(\min(r, k) + i)! \cdot (m - (\min(r, k) + i)!)}, \\ \text{Sing}(\mathcal{I}_{r,m \times n}^\sigma) &= \psi_{\mathcal{P}(\sigma)}^{-1}(\mathcal{M}_{r-1, m \times k}) \text{ if } r < \min(m, k), \text{ and empty otherwise.} \end{aligned} \quad (3.5)$$

Proof. The statements are an immediate consequence of Proposition 3.5 combined with Equations (2.26) and (2.27), and Fact 2.11. \square

We now consider the problem of finding an invariant matrix of low rank that is closest (with respect to the Euclidean distance) to a given matrix—or, more generally, squared-error loss minimization

$$\arg \min_{M \in \mathcal{I}_{r,m \times n}^\sigma} \|MX - Y\|_F^2. \quad (3.6)$$

We will see in Section 3.3 that there are linear neural networks whose function space is $\mathcal{I}_{r,m \times n}^\sigma$. Training such a network with the squared-error loss aims at solving (3.6).

Proposition 3.8. *For all matrices $X \in \mathbb{R}^{n \times d}$ and $Y \in \mathbb{R}^{m \times d}$ with $\text{rank}(XX^\top) = n$, squared-error loss minimization (3.6) can be solved using Eckart–Young on $\mathcal{M}_{\min(r,k), m \times k}(\mathbb{R})$, where k is the number of disjoint cycles in σ . In particular,*

$$\text{SEdegree}(\mathcal{I}_{r,m \times n}^\sigma) = \text{EDdegree}(\mathcal{I}_{r,m \times n}^\sigma) = \text{EDdegree}(\mathcal{M}_{\min(r,k), m \times k}) = \binom{\min(m, k)}{\min(r, k)}. \quad (3.7)$$

Proof. We make use of the linear isomorphism $\psi_{\mathcal{P}(\sigma)}$ from (3.3) that deletes columns of a given matrix M . For each set $A \in \mathcal{P}(\sigma)$, it keeps only one of the columns indexed by A . From the data matrix $X \in \mathbb{R}^{n \times d}$, we define a new matrix $\tilde{X} \in \mathbb{R}^{k \times d}$ by summing all the rows

of X that are indexed by the same set $A \in \mathcal{P}(\sigma)$. That way, we have $M \cdot X = \psi_{\mathcal{P}(\sigma)}(M) \cdot \tilde{X}$. Hence, minimizing the squared-error loss on $\mathcal{I}_{r,m \times n}^\sigma$ as in (3.6) is equivalent to solving

$$\arg \min_{\tilde{M} \in \mathcal{M}_{\min(r,k), m \times k}} \|\tilde{M}\tilde{X} - Y\|_F^2. \quad (3.8)$$

Note that $\tilde{X}\tilde{X}^\top$ is of full rank k since XX^\top is a full-rank matrix. Therefore, we can apply Lemma 2.3 and solve (3.8) via Eckart–Young as in Example 2.5. By choosing $X \in \mathbb{R}^{n \times n}$ to be either generic or the identity, we observe that (3.7) holds for the squared-error degree and the Euclidean distance degree of $\mathcal{I}_{r,m \times n}^\sigma$, respectively. \square

3.3 Parameterizing invariance and network design

In this section, we investigate which implications imposing invariance has on the individual layers of a linear autoencoder. Recall that a matrix $M \in \mathcal{M}_{m \times n}(\mathbb{K})$ has rank $r \leq \min(m, n)$ if and only if there exist rank- r matrices $A \in \mathcal{M}_{m \times r}(\mathbb{K})$ and $B \in \mathcal{M}_{r \times n}(\mathbb{K})$ such that $M = AB$. The factors of an invariant matrix do not need to be invariant, as the following example demonstrates. To be more precise, this question makes sense to be asked a priori only for the first layer, B , since the group G acts on \mathbb{R}^n only.

Example 3.9. Let $\sigma = (1\ 2) \in \mathcal{S}_3$ and consider

$$A = \begin{pmatrix} 1 & 1 \\ 1 & 1 \\ 0 & 0 \end{pmatrix} \quad \text{and} \quad B = \begin{pmatrix} 1 & 2 & 1 \\ 2 & 1 & 1 \end{pmatrix}. \quad (3.9)$$

Observe that B is not invariant under σ , but the product AB is. \diamond

Lemma 3.10 ([17, Proposition 22]). *Let $r \leq \min(m, n)$. Denote by*

$$\mu: \mathcal{M}_{m \times r} \times \mathcal{M}_{r \times n}, \quad (A, B) \mapsto A \cdot B, \quad (3.10)$$

the multiplication map. If $\text{rank}(M) = r$ and $M = \mu(A, B)$, then its fiber is

$$\mu^{-1}(M) = \{(AT^{-1}, TB) \mid T \in \text{GL}_r(\mathbb{K})\} \subset \mathcal{M}_{m \times r} \times \mathcal{M}_{r \times n}. \quad (3.11)$$

For $\sigma = \pi_1 \circ \dots \circ \pi_k \in \mathcal{S}_n$ with pairwise disjoint cycles π_i , we denote by $E_{\mathcal{P}(\sigma)}$ the $k \times n$ matrix that has the i -th standard basis vector $e_i \in \mathbb{R}^k$ in column j for all $j \in A_i$, $i = 1, \dots, k$. In particular, e_i occurs $\text{length}(\pi_i)$ many times as a column of $E_{\mathcal{P}(\sigma)}$, and $\text{rank}(E_{\mathcal{P}(\sigma)}) = k$.

Lemma 3.11. *Right-multiplication with $E_{\mathcal{P}(\sigma)}$ is precisely the inverse of the linear isomorphism $\psi_{\mathcal{P}(\sigma)}$ from (3.3). In other words, any matrix $M \in \mathcal{I}_{m \times n}^\sigma$ factorizes as*

$$M = \psi_{\mathcal{P}(\sigma)}(M) \cdot E_{\mathcal{P}(\sigma)}. \quad (3.12)$$

Proof. Let M be invariant under $\sigma \in \mathcal{S}_n$. For each $A_i \in \mathcal{P}(\sigma)$, the map $\psi_{\mathcal{P}(\sigma)}$ remembers one of the columns indexed by A_i , and collects them as the columns of the $m \times k$ matrix $\psi_{\mathcal{P}(\sigma)}(M)$. The remaining columns of M are copies of the columns of $\psi_{\mathcal{P}(\sigma)}(M)$. The repetition pattern is encoded in $E_{\mathcal{P}(\sigma)}$. \square

Example 3.12 ($n = 4$). Let $\sigma = (13)(2)(4) \in \mathcal{S}_4$, so that $k = 3$. The matrix

$$M = \begin{pmatrix} 1 & 0 & 1 & 1 \\ 2 & 4 & 2 & 1 \\ 3 & 4 & 3 & 1 \\ 0 & 2 & 0 & 1 \end{pmatrix} = \begin{pmatrix} 1 & 0 & 1 \\ 2 & 4 & 1 \\ 3 & 4 & 1 \\ 0 & 2 & 1 \end{pmatrix} \cdot \underbrace{\begin{pmatrix} 1 & 0 & 1 & 0 \\ 0 & 1 & 0 & 0 \\ 0 & 0 & 0 & 1 \end{pmatrix}}_{= E_{\{\{1,3\},\{2\},\{4\}\}}} \quad (3.13)$$

is invariant under σ and factorizes as claimed in Lemma 3.11. \diamond

Proposition 3.13. *Let $\sigma \in \mathcal{S}_n$ be decomposable into k pairwise disjoint cycles with $k \leq m$. Then the two-layer factorizations of the matrices in $\mathcal{I}_{m \times n}^\sigma$ that have the maximal possible rank k are precisely those factorizations whose first layer is invariant under σ . In symbols,*

$$\begin{aligned} & \{(A, B) \in \mathcal{M}_{m \times k} \times \mathcal{M}_{k \times n} \mid AB \in \mathcal{I}_{m \times n}^\sigma, \text{rank}(AB) = k\} \\ & = \{A \in \mathcal{M}_{m \times k} \mid \text{rank}(A) = k\} \times \{T \cdot E_{\mathcal{P}(\sigma)} \mid T \in \text{GL}_k\}. \end{aligned} \quad (3.14)$$

Proof. For $A \in \mathcal{M}_{m \times k}$ of full rank k and $T \in \text{GL}_k$, the product $ATE_{\mathcal{P}(\sigma)}$ has rank k and is invariant under σ by Lemma 3.11. For the converse direction, consider (A, B) as in the first row of (3.14). Since the product AB has rank k , both factors A and B must be of full rank. By Lemma 3.11, we have that $AB = \psi_{\mathcal{P}(\sigma)}(AB) \cdot E_{\mathcal{P}(\sigma)}$. Moreover, Lemma 3.10 implies that $(A, B) = (\psi_{\mathcal{P}(\sigma)}(AB)T^{-1}, TE_{\mathcal{P}(\sigma)})$ for some $T \in \text{GL}_k$. \square

This tells us that linear autoencoders are well-suited for expressing invariance when one imposes appropriate weight-sharing on the encoder. More precisely, the decoder factor A in (3.14) is an arbitrary full-rank matrix, but the encoder factor $T \cdot E_{\mathcal{P}(\sigma)}$ has repeated columns. We impose this repetition pattern via weight-sharing on the encoder. Proposition 3.13 states that invariant matrices naturally lie in the function space of such an autoencoder.

Definition 3.14. Given any permutation $\sigma \in \mathcal{S}_n$, we say that an encoder $\mathbb{R}^n \rightarrow \mathbb{R}^r$ has σ -weight-sharing if its representing matrices satisfy the following: for every set $S \in \mathcal{P}(\sigma)$, the columns indexed by the elements in S coincide, and no additional weight-sharing is imposed.

Example 3.15. We revisit Example 2.17. The invariance of a matrix $M = A \cdot B \in \mathcal{I}_{2,5 \times 5}^\sigma$ forces the encoder factor B to fulfill the weight-sharing property depicted in Figure 2. Which weights have to coincide is to be read from the color labeling in the figure. \diamond

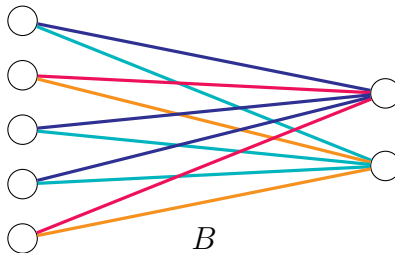


Figure 2: The σ -weight-sharing property imposed on the encoder by $\sigma = (134)(25)$.

Proposition 3.16. *Let $\sigma \in \mathcal{S}_n$ be a permutation consisting of k disjoint cycles with $k \leq m$, and let $r \leq k$. Consider the linear network $\mathbb{R}^n \rightarrow \mathbb{R}^r \rightarrow \mathbb{R}^m$ with two fully-connected layers and σ -weight-sharing imposed on the first layer $\mathbb{R}^n \rightarrow \mathbb{R}^r$. Its function space is $\mathcal{I}_{r,m \times n}^\sigma(\mathbb{R})$.*

Proof. Every matrix in the function space of the network is of the form AB such that the first-layer factor $B \in \mathcal{M}_{r \times n}$ has repeated columns according to $\mathcal{P}(\sigma)$. Therefore, the product AB has the same repetition in its columns, i.e., $AB \in \mathcal{I}_{m \times n}^\sigma$. Since $\text{rank}(AB) \leq \text{rank}(B) \leq r$, we conclude that $AB \in \mathcal{I}_{r,m \times n}^\sigma(\mathbb{R})$. For the converse direction, consider $M \in \mathcal{I}_{r,m \times n}^\sigma(\mathbb{R})$. By Lemma 3.11, that matrix can be factorized as $M = \psi_{\mathcal{P}(\sigma)}(M) \cdot E_{\mathcal{P}(\sigma)}$. If $r = k$, that factorization is compatible with the network and we are done. Thus, it is left to consider the case $r < k$. Note that $E_{\mathcal{P}(\sigma)}$ has full rank k by construction since the standard basis vectors in the columns of that matrix correspond to the k cycles of σ . Hence, we have that $\text{rank}(\psi_{\mathcal{P}(\sigma)}(M)) = \text{rank}(M) \leq r$. Therefore, we can factorize $\psi_{\mathcal{P}(\sigma)}(M) = A'B'$, where $A' \in \mathcal{M}_{m \times r}$ and $B' \in \mathcal{M}_{r \times k}$. The factorization $M = A' \cdot (B' \cdot E_{\mathcal{P}(\sigma)})$ is compatible with the network. \square

3.4 Induced filtration of $\mathcal{M}_{r,m \times n}$

If an $m \times n$ matrix M is invariant under $\sigma \in \mathcal{S}_n$, then it is also invariant under every permutation $\eta \in \mathcal{S}_n$ whose associated partition $\mathcal{P}(\eta)$ of $[n]$ is a refinement $\mathcal{P}(\eta) \prec \mathcal{P}(\sigma)$ of $\mathcal{P}(\sigma)$. This induces a filtration $\mathcal{I}_{m \times n}^\bullet$ of the variety $\mathcal{M}_{m \times n}$, which is indexed by partitions of $[n]$, and by intersecting with $\mathcal{M}_{r,m \times n}$, we obtain a filtration $\mathcal{I}_{r,m \times n}^\bullet$ of the variety $\mathcal{M}_{r,m \times n}$. The set $\mathcal{P}([n])$ of partitions of $[n]$ equals \mathcal{S}_n / \sim , where we identify $\sigma_1 \sim \sigma_2$ if and only if $\mathcal{P}(\sigma_1) = \mathcal{P}(\sigma_2)$. Here, $\mathcal{I}_{r,m \times n}^\mathcal{P}$ denotes any $\mathcal{I}_{r,m \times n}^\sigma$ for which $\mathcal{P}(\sigma) = \mathcal{P}$. As we saw earlier on, the variety $\mathcal{I}_{r,m \times n}^\sigma$ depends only on $\mathcal{P}(\sigma)$, but not on σ itself, hence this notion is well-defined. Together with refinements of partitions, the set of partitions of $[n]$ is a partially ordered set. Define the category $\underline{\text{Part}}_{[n]}^\prec$ whose set of objects is $\mathcal{P}([n])$, and a morphism from \mathcal{P}_1 to \mathcal{P}_2 whenever $\mathcal{P}_1 \prec \mathcal{P}_2$. By $\underline{\text{Subv}}_{\mathcal{M}_{r,m \times n}}^\subset$, we denote the category whose objects are subvarieties of $\mathcal{M}_{r,m \times n}$, and the inclusion as morphism between $U_1, U_2 \in \underline{\text{Subv}}_{\mathcal{M}_{r,m \times n}}^\subset$ whenever $U_1 \subset U_2$. This formulation gives rise to the functor

$$\underline{\text{Part}}_{[n]}^\prec \longrightarrow \underline{\text{Subv}}_{\mathcal{M}_{r,m \times n}}^\subset, \quad \mathcal{P} \mapsto \mathcal{I}_{r,m \times n}^\mathcal{P}. \quad (3.15)$$

Remark 3.17. The opposite category $\underline{\text{Part}}_{[n]}^{\prec, \text{op}}$ of $\underline{\text{Part}}_{[n]}^\prec$ is $\underline{\text{Part}}_{[n]}^\succ$, i.e., partitions of $[n]$ with coarsenings \succ of partitions as morphisms. In this formulation, the finest common coarsening of partitions $\mathcal{P}_1, \dots, \mathcal{P}_k$ then is their inverse limit. \diamond

4 Equivariance under cyclic subgroups of \mathcal{S}_n

In this section, we address equivariance under cyclic subgroups $G = \langle \sigma \rangle \leq \mathcal{S}_n$. We explore the irreducible components of the algebraic variety $\mathcal{E}_{r,n \times n}^\sigma \subset \mathcal{M}_{r,n \times n}$, both over \mathbb{R} and over \mathbb{C} , and quantities such as their dimensions, degrees, and singular loci. We parameterize the real components via autoencoders and discuss minimizing both the squared-error loss and the standard Euclidean distance on such a component.

4.1 Characterizing equivariance

We consider a permutation $\sigma = \pi_1 \circ \dots \circ \pi_k \in \mathcal{S}_n$ with a decomposition into pairwise disjoint cycles of lengths ℓ_1, \dots, ℓ_k . We reorder the entries in \mathbb{R}^n as in Step 1 of Procedure 2.16 such that the permutation matrix P_σ becomes block diagonal with cyclic blocks as in (2.32). Those square blocks have sizes ℓ_1, \dots, ℓ_k .

We are interested in matrices $M \in \mathcal{M}_{n \times n}$ that are equivariant under σ . For that, we divide $M \in \mathcal{M}_{n \times n}$ into blocks following the same pattern as in P_σ : M has square diagonal blocks $M^{(ii)}$ of size $\ell_i \times \ell_i$ and rectangular off-diagonal blocks $M^{(ij)}$ of size $\ell_i \times \ell_j$. We now show that the equivariance of M under σ means that its blocks have to be (*rectangular*) *circulant matrices*. We can observe this property in our previous example (2.13). We call a (possibly non-square) matrix *circulant* if each row is a copy of the previous row, cyclically shifted one step to the right, and also each column is a copy of the previous column, cyclically shifted one step downwards. Some examples of such matrices are shown in Equation (4.1). A circulant matrix of size $\ell_i \times \ell_j$ has at most $\gcd(\ell_i, \ell_j)$ different entries.

$$\begin{aligned} & \begin{pmatrix} \alpha^{(ij)} & \beta^{(ij)} & \gamma^{(ij)} \\ \gamma^{(ij)} & \alpha^{(ij)} & \beta^{(ij)} \\ \beta^{(ij)} & \gamma^{(ij)} & \alpha^{(ij)} \end{pmatrix}, \quad \begin{pmatrix} \alpha^{(ij)} & \alpha^{(ij)} & \alpha^{(ij)} \\ \alpha^{(ij)} & \alpha^{(ij)} & \alpha^{(ij)} \\ \alpha^{(ij)} & \alpha^{(ij)} & \alpha^{(ij)} \end{pmatrix}, \\ & \begin{pmatrix} \alpha^{(ij)} & \alpha^{(ij)} & \alpha^{(ij)} \\ \alpha^{(ij)} & \alpha^{(ij)} & \alpha^{(ij)} \end{pmatrix}, \quad \begin{pmatrix} \alpha^{(ij)} & \beta^{(ij)} & \alpha^{(ij)} & \beta^{(ij)} \\ \beta^{(ij)} & \alpha^{(ij)} & \beta^{(ij)} & \alpha^{(ij)} \end{pmatrix}. \end{aligned} \tag{4.1}$$

Proposition 4.1. *The matrix $M \in \mathcal{M}_{n \times n}$ is equivariant under σ if and only if each block $M^{(ij)}$ of M is a (possibly non-square) circulant matrix.*

Proof. Since P_σ is a block diagonal matrix with cyclic blocks C_1, \dots, C_k , the equivariance condition $MP = PM$ means that $M^{(ij)}C_j = C_iM^{(ij)}$ for all i, j . The multiplication by C_i from the left cyclically permutes the rows of M , and the multiplication by C_j from the right permutes the columns of M . Since the resulting matrices need to coincide, it follows that the block $M^{(ij)}$ has to be circulant. \square

4.1.1 Irreducible components of $\mathcal{E}_{r, n \times n}^\sigma(\mathbb{C})$

Our focus now shifts to exploring the intriguing algebraic properties arising from the intersection of the determinantal variety $\mathcal{M}_{r, n \times n}$ with the linear space $C(P_\sigma) = \mathcal{E}_{n \times n}^\sigma$. Their intersection $\mathcal{E}_{r, n \times n}^\sigma = \mathcal{M}_{r, n \times n} \cap C(P_\sigma)$ is an algebraic set that is, in general, reducible. In the following statement, we use the notation from Lemma 2.19.

Theorem 4.2. *There is a one-to-one correspondence between the irreducible components of $\mathcal{E}_{r, n \times n}^\sigma(\mathbb{C})$ and the non-negative integer solutions $\mathbf{r} = (r_{l,m})$ of*

$$\sum_{l \geq 1} \sum_{m \in (\mathbb{Z}/l\mathbb{Z})^\times} r_{l,m} = r, \quad \text{where } 0 \leq r_{l,m} \leq d_l. \tag{4.2}$$

The irreducible component $\mathcal{E}_{r,n \times n}^{\sigma, \mathbf{r}}(\mathbb{C})$ corresponding to such an integer solution \mathbf{r} after the base change from Procedure 2.16 is the following direct product of determinantal varieties:

$$\prod_{l \geq 1} \prod_{m \in (\mathbb{Z}/l\mathbb{Z})^\times} \mathcal{M}_{r_{l,m}, d_l \times d_l}(\mathbb{C}). \quad (4.3)$$

Proof. By Lemma 2.19 (and its proof), every matrix $M \in C(P_\sigma)$ is similar to a complex block diagonal matrix B with $\varphi(l) = |(\mathbb{Z}/l\mathbb{Z})^\times|$ many blocks of size $d_l \times d_l$ for every l . We will denote these blocks by $B_{l,m}$ for $m \in (\mathbb{Z}/l\mathbb{Z})^\times$. Imposing a rank constraint on the matrix M affects the rank of the diagonal blocks of B . Hence, if $r_{l,m}$ is the rank of the block $B_{l,m}$, then M has rank r if and only if (4.2) holds. This implies that the number of different irreducible components of $\mathcal{E}_{r,n \times n}^\sigma(\mathbb{C})$ is exactly the number of integer solution vectors to (4.2). \square

Example 4.3. Let σ again denote the clockwise rotation by 90 degrees on images with 3×3 pixels. The numbers d_l are computed in Example 2.23. For the permutation matrix in (2.11) and $r = 3$, the number of irreducible components is equal to the number of non-negative integer solutions of the equation $r_{1,1} + r_{2,1} + r_{4,1} + r_{4,3} = 3$, where $r_{1,1} \leq 3 = d_1$, $r_{2,1} \leq 2 = d_2$, and $r_{4,1}, r_{4,3} \leq 2 = d_4$. With the stars and bars formula, one finds that there are $\binom{6}{3} - 3 = 17$ solutions, and hence $\mathcal{E}_{3,9 \times 9}^\sigma(\mathbb{C})$ has 17 irreducible components, as seen in Example 2.23. Six of those have dimension 11, five have dimension 9, and the remaining six have dimension 7. The six maximal-dimensional components correspond to the integer solutions $(r_{1,1}, r_{2,1}, r_{4,1}, r_{4,3}) \in \{(2, 1, 0, 0), (2, 0, 1, 0), (2, 0, 0, 1), (1, 1, 1, 0), (1, 1, 0, 1), (1, 0, 1, 1)\}$. \diamond

These discussions imply that, in contrast to the case of invariance, autoencoders are not well-suited to parameterize *all* equivariant functions: For a rank constraint $r < n$, $\mathcal{E}_{r,n \times n}^\sigma$ has many components; the function space of an autoencoder would cover at most one of them.

Not all irreducible components of $\mathcal{E}_{r,n \times n}^\sigma(\mathbb{C})$ have to appear in the real locus $\mathcal{E}_{r,n \times n}^\sigma(\mathbb{R})$. We will describe the real components in Section 4.1.2. We now describe some algebraic properties of the complex component $\mathcal{E}_{r,n \times n}^{\sigma, \mathbf{r}}(\mathbb{C})$.

Proposition 4.4. *Let \mathbf{r} be an integer solution of (4.2). Then,*

$$\begin{aligned} \dim(\mathcal{E}_{r,n \times n}^{\sigma, \mathbf{r}}(\mathbb{C})) &= \sum_{l \geq 1} \sum_{m \in (\mathbb{Z}/l\mathbb{Z})^\times} (2d_l - r_{l,m}) \cdot r_{l,m}, \\ \deg(\mathcal{E}_{r,n \times n}^{\sigma, \mathbf{r}}(\mathbb{C})) &= \prod_l \prod_{m \in (\mathbb{Z}/l\mathbb{Z})^\times} \prod_{i=0}^{d_l - r_{l,m} - 1} \frac{(d_l + i)! \cdot i!}{(r_{l,m} + i)! \cdot (d_l - r_{l,m} + i)!}, \\ \text{Sing}(\mathcal{E}_{r,n \times n}^{\sigma, \mathbf{r}}(\mathbb{C})) &= \mathcal{E}_{r,n \times n}^{\sigma, \mathbf{r}}(\mathbb{C}) \cap \mathcal{E}_{r-1,n \times n}^\sigma(\mathbb{C}) \text{ if } r < n, \text{ and empty otherwise.} \end{aligned} \quad (4.4)$$

In particular, the locus of singular points of $\mathcal{E}_{r,n \times n}^\sigma(\mathbb{C})$ is $\mathcal{E}_{r-1,n \times n}^\sigma(\mathbb{C})$.

Proof. Due to Lemma 2.12, we can read off the dimension, degree, and singular locus of $\mathcal{E}_{r,n \times n}^{\sigma, \mathbf{r}}(\mathbb{C})$ from (4.3). The first two statements follow directly from (2.26) and (2.27). If $r = n$, then $\mathcal{E}_{r,n \times n}^\sigma(\mathbb{C})$ is a linear space and thus smooth. Otherwise, by Fact 2.11, the singular locus of (4.3) is its intersection with $\mathcal{M}_{r-1,n \times n}(\mathbb{C})$. Now, Lemma 2.12 implies

that the singular locus of $\mathcal{E}_{r,n \times n}^{\sigma, \mathbf{r}}(\mathbb{C})$ is $\mathcal{E}_{r,n \times n}^{\sigma, \mathbf{r}}(\mathbb{C}) \cap \mathcal{M}_{r-1, n \times n}(\mathbb{C}) = \mathcal{E}_{r,n \times n}^{\sigma, \mathbf{r}}(\mathbb{C}) \cap \mathcal{E}_{r-1, n \times n}^{\sigma}(\mathbb{C})$. Finally, since the intersection of two distinct components $\mathcal{E}_{r,n \times n}^{\sigma, \mathbf{r}}(\mathbb{C})$ and $\mathcal{E}_{r,n \times n}^{\sigma, \mathbf{r}'}(\mathbb{C})$ is a subset of $\mathcal{E}_{r-1, n \times n}^{\sigma}(\mathbb{C})$, we get that

$$\text{Sing}(\mathcal{E}_{r,n \times n}^{\sigma}(\mathbb{C})) = \bigcup_{\mathbf{r}} (\mathcal{E}_{r,n \times n}^{\sigma, \mathbf{r}}(\mathbb{C}) \cap \mathcal{E}_{r-1, n \times n}^{\sigma}(\mathbb{C})) = \mathcal{E}_{r-1, n \times n}^{\sigma}(\mathbb{C}), \quad (4.5)$$

concluding the proof. \square

4.1.2 Irreducible components of $\mathcal{E}_{r,n \times n}^{\sigma}(\mathbb{R})$

To obtain the real components of $\mathcal{E}_{r,n \times n}^{\sigma}(\mathbb{R})$, we introduce an orthonormal basis Q_{σ} in which the permutation matrix P_{σ} becomes a real block diagonal matrix of a certain type. This will allow us to compute the commutator of $P_{\sigma}^{\sim Q_{\sigma}}$ while preserving the imposed rank constraint.

Recall that for any given circulant matrix $C \in \mathcal{M}_{n \times n}(\mathbb{R})$, the vectors

$$v_j = (1, \zeta_n^j, \zeta_n^{2j}, \dots, \zeta_n^{(n-1)j})^{\top}, \quad j = 0, \dots, n-1, \quad (4.6)$$

are eigenvectors of C , where $\zeta_n = e^{2\pi i/n}$. In the basis $\{v_0, \dots, v_{n-1}\}$, the matrix C becomes a complex diagonal matrix. Now, let $v_{-j} := v_{n-j} = \overline{v_j}$ and consider the following real vectors

$$w_0 := \frac{1}{\sqrt{n}}v_0, \quad w_j := \frac{1}{\sqrt{2n}}(v_j + v_{-j}), \quad w_{-j} := \frac{1}{\sqrt{2ni}}(v_j - v_{-j}). \quad (4.7)$$

The vectors w_j with $-n/2 < j \leq \lfloor n/2 \rfloor$ form a basis. We reorder them so that w_j and w_{-j} are next to each other. The resulting basis transforms the matrix C into a real block diagonal form. Each block has size at most 2, where scalar blocks represent the real eigenvalues, and 2×2 blocks are scaled rotation matrices of the form

$$\begin{pmatrix} \Re(\lambda_j) & -\Im(\lambda_j) \\ \Im(\lambda_j) & \Re(\lambda_j) \end{pmatrix}, \quad (4.8)$$

where λ_j is a complex eigenvalue of C . Since

$$v_l^{\top} v_k = \begin{cases} n & \text{if } l = -k, \\ 0 & \text{if } l \neq \pm k, \end{cases} \quad (4.9)$$

the vectors w_j form an orthonormal basis.

Now let P_{σ} be a permutation matrix arranged in block form, with cyclic matrices C_k having sizes $\ell_k \times \ell_k$ as blocks—each corresponding to a cycle of σ . Leveraging the orthonormal basis crafted from the vectors of (4.7), we transform each C_k into a block diagonal matrix, with each block being square of size at most 2. This transformation is captured by an orthonormal base change denoted by $Q_{\sigma}^{(1)}$. By a further orthonormal base change, $Q_{\sigma}^{(2)}$, we group equal blocks. We denote the total full base change via the orthogonal matrix $Q_{\sigma}^{(2)}Q_{\sigma}^{(1)}$ by Q_{σ} and we call it *realization base change* of P_{σ} .

Example 4.5. For the rotation of 3×3 images by 90 degrees, the permutation $\sigma \in \mathcal{S}_9$ decomposes into two cycles of length 4, and one of length 1. The matrix $P_\sigma^{\sim T_1}$, with a permutation matrix T_1 as in Procedure 2.16, has two circulant 4×4 blocks, and one scalar block. As basis for the 4×4 blocks, we consider

$$(1 \ 1 \ 1 \ 1)^\top, (1 \ -1 \ 1 \ -1)^\top, \Re(1 \ i \ -1 \ -i)^\top, \Im(1 \ i \ -1 \ -i)^\top \quad (4.10)$$

and, after scaling to make them orthonormal, collect these vectors in the orthogonal matrix

$$O = \frac{1}{2} \cdot \begin{pmatrix} 1 & 1 & \sqrt{2} & 0 \\ 1 & -1 & 0 & \sqrt{2} \\ 1 & 1 & -\sqrt{2} & 0 \\ 1 & -1 & 0 & -\sqrt{2} \end{pmatrix}. \quad (4.11)$$

A base change via the 9×9 matrix

$$Q_\sigma^{(1)} = \left(\begin{array}{c|c|c} O & 0 & 0 \\ \hline 0 & O & 0 \\ \hline 0 & 0 & 1 \end{array} \right) \quad (4.12)$$

brings $P_\sigma^{\sim T_1}$ into the desired form with scaled rotation matrices as blocks, namely

$$\begin{pmatrix} 1 & & & & & & & & \\ & -1 & & & & & & & \\ & & 0 & -1 & & & & & \\ & & 1 & 0 & & & & & \\ \hline & & & & 1 & & & & \\ & & & & & -1 & & & \\ & & 0 & & & 0 & -1 & & \\ & & & & & 1 & 0 & & \\ \hline & & & & & & & & 1 \end{pmatrix}. \quad (4.13)$$

A further orthogonal base change $Q_\sigma^{(2)}$ via grouping identical blocks in (4.13) brings the matrix into the block diagonal form $I_3 \oplus (-I_2) \oplus \begin{pmatrix} 0 & -1 \\ 1 & 0 \end{pmatrix} \oplus \begin{pmatrix} 0 & -1 \\ 1 & 0 \end{pmatrix}$. From this particularly nice form, one reads that matrices that commute with it have to be of the form

$$\begin{pmatrix} \alpha_{11} & \alpha_{12} & \alpha_{13} & & & & & & \\ \alpha_{21} & \alpha_{22} & \alpha_{23} & & 0 & & & & 0 \\ \alpha_{31} & \alpha_{32} & \alpha_{33} & & & & & & \\ \hline & & & \beta_{12} & \beta_{22} & & & & 0 \\ & & 0 & \beta_{21} & \beta_{23} & & & & \\ \hline & & & & & \gamma_1 & -\gamma_2 & \delta_1 & -\delta_2 \\ & & 0 & & 0 & \gamma_2 & \gamma_1 & \delta_2 & \delta_1 \\ & & & & & \epsilon_1 & -\epsilon_2 & \eta_1 & -\eta_2 \\ & & & & & \epsilon_2 & \epsilon_1 & \eta_2 & \eta_1 \end{pmatrix}. \quad (4.14)$$

The pattern observed here will extend to the general case. Since the last 4×4 block in (4.14) can only have rank 0, 2, or 4 over \mathbb{R} , there are five ways how the matrix (4.14) can be of rank 3. These five irreducible components of $\mathcal{E}_{3,9 \times 9}^\sigma$, that were already mentioned in Section 2.1.2, are listed in Example 4.9. \diamond

Our next step involves finding the commutator of $P_\sigma^{\sim Q_\sigma}$ in general, and subsequently imposing the rank constraint. To achieve this, we will make use of the following isomorphism of rings, to which we refer as *realization*:

$$\mathcal{R}: \mathbb{C} \longrightarrow \left\{ \begin{pmatrix} a & -b \\ b & a \end{pmatrix} \mid a, b \in \mathbb{R} \right\}, \quad a + ib \mapsto \begin{pmatrix} a & -b \\ b & a \end{pmatrix}. \quad (4.15)$$

Definition 4.6. Let $Z = [z_{ij}]_{ij}$ be a complex $m \times n$ matrix. We define the *realization of Z* to be the real $2m \times 2n$ matrix $\mathcal{R}(Z)$, where entry-wise application of \mathcal{R} is meant.

In other words, the realization of Z is the matrix in $\mathcal{M}_{2m \times 2n}(\mathbb{R})$ whose (i, j) -th block is

$$\mathcal{R}(z_{ij}) = \begin{pmatrix} \Re(z_{ij}) & -\Im(z_{ij}) \\ \Im(z_{ij}) & \Re(z_{ij}) \end{pmatrix}. \quad (4.16)$$

We denote the space of such real matrices by $\mathcal{R}(\mathcal{M}_{m \times n}(\mathbb{C}))$. The realization space $\mathcal{R}(\mathcal{M}_{r, m \times n}(\mathbb{C}))$ is then precisely the set of matrices in $\mathcal{R}(\mathcal{M}_{m \times n}(\mathbb{C}))$ of rank at most $2r$. Note that $\dim_{\mathbb{R}} \mathcal{R}(\mathcal{M}_{r, m \times n}(\mathbb{C})) = 2 \cdot \dim_{\mathbb{C}} \mathcal{M}_{r, m \times n}(\mathbb{C})$.

Lemma 4.7. Let $z \in \mathbb{C}$ be non-real. Then the real commutator of the matrix $\bigoplus_{j=1}^m \mathcal{R}(z)$ is

$$C_{\mathbb{R}} \left(\bigoplus_{j=1}^m \mathcal{R}(z) \right) = \mathcal{R}(\mathcal{M}_{m \times m}(\mathbb{C})). \quad (4.17)$$

Proof. Let $M = [M_{i,j}]_{i,j}$ be a matrix in $\mathcal{M}_{2m \times 2m}(\mathbb{R})$ with 2×2 blocks $M_{i,j}$. Note that M commutes with $\bigoplus_{j=1}^m \mathcal{R}(z)$ if and only if every block $M_{i,j}$ commutes with $\mathcal{R}(z)$. Since z is non-real, the commutator of $\mathcal{R}(z)$ is exactly the set of scaled rotation matrices. Hence, $C_{\mathbb{R}}(\bigoplus_{j=1}^m \mathcal{R}(z))$ is equal to the realization of $\mathcal{M}_{m \times m}(\mathbb{C})$. \square

Theorem 4.8. There is a one-to-one correspondence between the irreducible components of $\mathcal{E}_{r, n \times n}^\sigma(\mathbb{R})$ that contain a matrix of rank r and the non-negative integer solutions $\mathbf{r} = (r_{l,m})$ of

$$r_{1,1} + r_{2,1} + \sum_{l \geq 3} \sum_{\substack{m \in (\mathbb{Z}/l\mathbb{Z})^\times \\ \frac{1}{2} < \frac{m}{l} < 1}} 2 \cdot r_{l,m} = r, \quad \text{where } 0 \leq r_{l,m} \leq d_l. \quad (4.18)$$

The irreducible component $\mathcal{E}_{r, n \times n}^{\sigma, \mathbf{r}}(\mathbb{R})$ corresponding to such an integer solution \mathbf{r} after the base change Q_σ is

$$\mathcal{M}_{r_{1,1}, d_1 \times d_1}(\mathbb{R}) \times \mathcal{M}_{r_{2,1}, d_2 \times d_2}(\mathbb{R}) \times \prod_{l \geq 3} \prod_{\substack{m \in (\mathbb{Z}/l\mathbb{Z})^\times \\ \frac{1}{2} < \frac{m}{l} < 1}} \mathcal{R}(\mathcal{M}_{r_{l,m}, d_l \times d_l}(\mathbb{C})). \quad (4.19)$$

Proof. By Lemma 2.15, we have that $C_{\mathbb{R}}(P_\sigma^{\sim Q_\sigma}) = (C_{\mathbb{R}}(P_\sigma))^{\sim Q_\sigma} = (\mathcal{E}_{n \times n}^\sigma(\mathbb{R}))^{\sim Q_\sigma}$. Also, Lemma 2.18 implies that the commutator of $P_\sigma^{\sim Q_\sigma}$ is the set of block diagonal matrices $R = \bigoplus_{m,l} R_{l,m}$, where the direct sum is running over $m \in (\mathbb{Z}/l\mathbb{Z})^\times$ and $\{l \mid \frac{1}{2} \leq \frac{m}{l} \leq 1\}$,

such that $R_{1,1}$ and $R_{2,1}$ are arbitrary matrices of size $d_1 \times d_1$ and $d_2 \times d_2$, respectively. For the other pairs (l, m) with $\frac{1}{2} < \frac{m}{l} < 1$ and $\gcd(l, m) = 1$, Lemma 4.7 implies that the matrix $R_{l,m}$ is an arbitrary matrix in $\mathcal{R}(\mathcal{M}_{d_l \times d_l}(\mathbb{C}))$. Now, note that for a complex matrix Z , we have $\text{rank}_{\mathbb{R}}(\mathcal{R}(Z)) = 2 \cdot \text{rank}_{\mathbb{C}}(Z)$. Hence, imposing the rank constraint leads to (4.18), and the corresponding irreducible component can be seen in (4.19). \square

Example 4.9. For rotating 3×3 images by 90 degrees, the permutation $\sigma \in \mathcal{S}_9$ decomposes into two cycles of length 4, and one of length 1. Then $P_{\sigma}^{\sim Q_{\sigma}}$ is the block diagonal matrix $\mathbb{I}_3 \oplus (-\mathbb{I}_2) \oplus [\mathcal{R}(i) \oplus \mathcal{R}(i)]$. Thus, the commutator of $P_{\sigma}^{\sim Q_{\sigma}}$ is equal to $\mathcal{M}_{3 \times 3}(\mathbb{R}) \oplus \mathcal{M}_{2 \times 2}(\mathbb{R}) \oplus \mathcal{R}(\mathcal{M}_{2 \times 2}(\mathbb{C}))$. The matrix in (4.14) is an example of an element of that space. For $r = 3$, the number of real irreducible components matches the non-negative integer solutions of the equation $r_{1,1} + r_{2,1} + 2 \cdot r_{4,3} = 3$. Here, $r_{1,1} \leq 3 = d_1$, $r_{2,1} \leq 2 = d_2$, and $r_{4,3} \leq 2 = d_4$. Solving the equation yields five solutions: $(3, 0, 0)$, $(2, 1, 0)$, $(1, 2, 0)$, $(1, 0, 1)$, and $(0, 1, 1)$. This is a notable decrease of the number of complex irreducible components from 17 in Example 4.3 to 5. The dimensions of the 5 real components are 9, 11, 9, 11, and 9. \diamond

We can compute the dimensions of the real components of $\mathcal{E}_{r,n \times n}^{\sigma}$ in a similar fashion as the complex components; see Proposition 4.12. For the singular loci of the real components, we make use of the following observation. Recall that for a given holomorphic function $f : \mathbb{C}^n \rightarrow \mathbb{C}$, we can write

$$f(z_1, \dots, z_n) = u(x_1, y_1, \dots, x_n, y_n) + i v(x_1, y_1, \dots, x_n, y_n), \quad (4.20)$$

where u and v are smooth real-valued functions and $z_j = x_j + iy_j$ for every j . The Cauchy–Riemann equations and Wirtinger derivatives provide the following relations:

$$\frac{\partial u}{\partial x_j} = \frac{\partial v}{\partial y_j} \quad \text{and} \quad \frac{\partial u}{\partial y_j} = -\frac{\partial v}{\partial x_j}, \quad (4.21)$$

and

$$\frac{\partial f}{\partial z_j} = \frac{1}{2} \left(\frac{\partial f}{\partial x_j} - i \frac{\partial f}{\partial y_j} \right) = \frac{\partial u}{\partial x_j} + i \frac{\partial v}{\partial x_j} \quad (4.22)$$

for all $j = 1, \dots, n$. Therefore, by (4.21) and (4.22), the Jacobian $\text{Jac}(u, v) = [\frac{\nabla u}{\nabla v}]$ can be simplified as follows:

$$\begin{aligned} \text{Jac}(u, v) &= \begin{bmatrix} \frac{\partial u}{\partial x_1} & \frac{\partial v}{\partial x_1} & \cdots & \frac{\partial u}{\partial x_n} & \frac{\partial v}{\partial x_n} \\ \frac{\partial u}{\partial y_1} & \frac{\partial v}{\partial y_1} & \cdots & \frac{\partial u}{\partial y_n} & \frac{\partial v}{\partial y_n} \end{bmatrix} = \mathcal{R} \left[\frac{\partial u}{\partial x_1} + i \frac{\partial v}{\partial x_1}, \dots, \frac{\partial u}{\partial x_n} + i \frac{\partial v}{\partial x_n} \right] \\ &= \mathcal{R} \left(\left[\frac{\partial f}{\partial x_1}, \dots, \frac{\partial f}{\partial x_n} \right] \right) = \mathcal{R} \left(\left[\frac{\partial f}{\partial z_1}, \dots, \frac{\partial f}{\partial z_n} \right] \right) = \mathcal{R}(\nabla f). \end{aligned} \quad (4.23)$$

Lemma 4.10. *Let $I \subset \mathbb{C}[z_1, \dots, z_n]$ be a prime ideal generated by polynomials f_1, \dots, f_k . We split $f_j = u_j + iv_j$ into their real and imaginary parts and denote by $J \subset \mathbb{R}[x_1, y_1, \dots, x_n, y_n]$ the ideal generated by the u_j 's and v_j 's. Then a point $\mathbf{z}_0 \in \mathbb{C}^n$ is singular for the complex variety $V(I)$ if and only if $(\mathbf{x}_0, \mathbf{y}_0) = (\Re(\mathbf{z}_0), \Im(\mathbf{z}_0))$ in \mathbb{R}^{2n} is singular for $V(J)$.*

Proof. By (4.23), for any $\mathbf{z}_0 \in \mathbb{C}^n$ and its counterpart $(\mathbf{x}_0, \mathbf{y}_0) \in \mathbb{R}^{2n}$, we have

$$\begin{aligned} \text{rank}_{\mathbb{R}} \text{Jac}_{(\mathbf{x}_0, \mathbf{y}_0)}(u_1, v_1, \dots, u_k, v_k) &= \text{rank}_{\mathbb{R}} \mathcal{R}(\text{Jac}_{\mathbf{z}_0}(f_1, \dots, f_k)) \\ &= 2 \cdot \text{rank}_{\mathbb{C}} \text{Jac}_{\mathbf{z}_0}(f_1, \dots, f_k). \end{aligned} \quad (4.24)$$

Note that a point $\mathbf{z}_0 \in \mathbb{C}^n$ (resp., $(\mathbf{x}_0, \mathbf{y}_0) \in \mathbb{R}^{2n}$) is singular for $V(I)$ (resp., $V(J)$) if and only if the rank of the Jacobian $\text{Jac}_{\mathbf{z}_0}(f_1, \dots, f_k)$ (resp., $\text{Jac}_{(\mathbf{x}_0, \mathbf{y}_0)}(u_1, v_1, \dots, u_k, v_k)$) drops. Hence, due to (4.24), \mathbf{z}_0 is singular for $V(I)$ if and only if $(\mathbf{x}_0, \mathbf{y}_0)$ is singular for $V(J)$. \square

Corollary 4.11. *Let $0 < r < \min(m, n)$. A matrix $M \in \mathcal{R}(\mathcal{M}_{r, m \times n}(\mathbb{C}))$ is a singular point of $\mathcal{R}(\mathcal{M}_{r, m \times n}(\mathbb{C}))$ if and only if $M \in \mathcal{R}(\mathcal{M}_{r-1, m \times n}(\mathbb{C}))$.*

Proof. Let $I = \langle f_1, \dots, f_k \rangle$ be the ideal of $\mathcal{M}_{r, m \times n}(\mathbb{C})$. Then the realization $\mathcal{R}(\mathcal{M}_{r, m \times n}(\mathbb{C}))$ is the common zero locus of $u_1, v_1, \dots, u_k, v_k$, where $f_j = u_j + iv_j$. By Fact 2.11, we know that $\text{Sing}(\mathcal{M}_{r, m \times n}(\mathbb{C})) = \mathcal{M}_{r-1, m \times n}(\mathbb{C})$, and thus Lemma 4.10 implies that $\text{Sing}(\mathcal{R}(\mathcal{M}_{r, m \times n}(\mathbb{C}))) = \mathcal{R}(\mathcal{M}_{r-1, m \times n}(\mathbb{C}))$. \square

Proposition 4.12. *Let \mathbf{r} be an integer solution of (4.18). The dimension of $\mathcal{E}_{r, n \times n}^{\sigma, \mathbf{r}}(\mathbb{R})$ is*

$$(2d_1 - r_{1,1}) \cdot r_{1,1} + (2d_2 - r_{2,1}) \cdot r_{2,1} + 2 \cdot \sum_{l \geq 3} \sum_{\substack{m \in (\mathbb{Z}/l\mathbb{Z})^\times, \\ \frac{1}{2} < \frac{m}{l} < 1}} (2d_l - r_{l,m}) \cdot r_{l,m}, \quad (4.25)$$

and its singular locus is

$$\text{Sing}(\mathcal{E}_{r, n \times n}^{\sigma, \mathbf{r}}(\mathbb{R})) = \mathcal{E}_{r, n \times n}^{\sigma, \mathbf{r}}(\mathbb{R}) \cap \mathcal{E}_{r-1, n \times n}^{\sigma, \mathbf{r}}(\mathbb{R}) \text{ if } r < n, \text{ and empty otherwise.} \quad (4.26)$$

Proof. As in the proof of Proposition 4.4, we make use of Lemma 2.12. Then, the first statement follows from (4.19), the fact that $\dim_{\mathbb{R}} \mathcal{R}(\mathcal{M}_{r, m \times n}(\mathbb{C})) = 2 \cdot \dim_{\mathbb{C}} \mathcal{M}_{r, m \times n}(\mathbb{C})$, and (2.26). If $r = n$, then $\mathcal{E}_{r, n \times n}^{\sigma, \mathbf{r}}(\mathbb{R})$ is a linear space and thus smooth. Otherwise, by Lemma 2.12 and Corollary 4.11, the singular locus of (4.19) is its intersection with $\mathcal{M}_{r-1, n \times n}$. Now, the second assertion follows from Lemma 2.12. \square

In light of Section 4.3, where we will show that each real irreducible component $\mathcal{E}_{r, n \times n}^{\sigma, \mathbf{r}}(\mathbb{R})$ is the function space of a σ -equivariant autoencoder, the second assertion of Proposition 4.12 means that the singular locus of the function space is the finite union of function spaces of networks with smaller architectures.

To give a degree formula for the real components of $\mathcal{E}_{r, n \times n}^{\sigma}$ as we did in the complex case in Proposition 4.4, we would need to have a formula for the degree of the realization space $\mathcal{R}(\mathcal{M}_{r, m \times n}(\mathbb{C})) \subset \mathbb{R}^{2m \times 2n}$. More precisely, for a well-defined notion of degree, we need to consider the degree of the Zariski closure of the real variety $\mathcal{R}(\mathcal{M}_{r, m \times n}(\mathbb{C}))$ inside $\mathbb{C}^{2m \times 2n}$. For that degree, we conjecture the following:

Conjecture 4.13. $\deg \mathcal{R}(\mathcal{M}_{r, m \times n}) = (\deg \mathcal{M}_{r, m \times n})^2$.

We validated the conjecture for $(m, n, r) = (1, 1, 1) \dots (3, 9, 8)$, $(4, 4, 2) \dots (4, 5, 5)$, $(5, 4, 2)$, $(5, 5, 1)$, $(6, 6, 1)$, $(6, 7, 1)$, $(7, 6, 1)$. To test Conjecture 4.13 for a specific choice of parameters (m, n, r) , one can run the following lines in Macaulay2, here displayed for $(m, n, r) = (3, 2, 1)$:

```

m = 3; n = 2; r = 1;
R1 = QQ[c_(1,1)..c_(m,n)];
M = matrix apply(toList(1..m), i -> apply(toList(1..n), j -> c_(i,j)));
I = minors(r+1,M);
R2 = QQ[a_(1,1)..a_(m,n),b_(1,1)..b_(m,n), x] / ideal(x^2+1);
f = map(R2, R1, flatten apply(toList(1..m),
i -> apply(toList(1..n), j -> a_(i,j) + x*b_(i,j))));
getRealAndImaginaryPart = eq -> (
eqReal = sub(eq, x=>0);
eqImag = sub((eq - eqReal)/x,R2);
{eqReal,eqImag}
);
J = ideal flatten apply(flatten entries gens I,
eq -> getRealAndImaginaryPart f eq);
R3 = QQ[a_(1,1)..a_(m,n),b_(1,1)..b_(m,n)];
degree sub(J,R3) == (degree I)^2

```

4.2 Squared-error loss minimization on $\mathcal{E}_{r,n \times n}^\sigma(\mathbb{R})$

The explicit structure of the space of equivariant linear maps in Theorem 4.8, with a bound on their rank imposed, provides an efficient algorithm to find the point M in $\mathcal{E}_{r,n \times n}^\sigma(\mathbb{R})$ that minimizes the squared-error loss. Given $X \in \mathbb{R}^{n \times d}$ with $\text{rank}(XX^\top) = n$ and $Y \in \mathbb{R}^{m \times d}$, our task is to find a point in $\mathcal{E}_{r,n \times n}^\sigma(\mathbb{R})$ that minimizes $\|MX - Y\|_F^2$. For autoencoders, the input data equals the output data, i.e., $Y = X$, but we here allow arbitrary output data Y . The following algorithm reduces this task to many instances of minimizing the standard Euclidean distance to rank-bounded matrices via Eckart–Young, which in particular shows $\text{SEdegree}(\mathcal{E}_{r,n \times n}^\sigma(\mathbb{R})) = \text{EDdegree}(\mathcal{E}_{r,n \times n}^\sigma(\mathbb{R}))$. We proceed with the following three steps, for each of which we give further details right after.

Step 1. *Transform the task to finding a block diagonal matrix $B \in (\mathcal{E}_{r,n \times n}^\sigma(\mathbb{R}))^{\sim Q_\sigma}$ that minimizes $\|B - U\|_{\tilde{X}\tilde{X}^\top}^2$, where $\tilde{X} := Q_\sigma^\top X$ and $U := Q_\sigma^\top Y \tilde{X}^\top (\tilde{X}\tilde{X}^\top)^{-1}$.*

Due to the orthogonality of Q_σ , we see as in (2.31) that $\|MX - Y\|_F^2 = \|Q_\sigma^\top MX - Q_\sigma^\top Y\|_F^2 = \|M^{\sim Q_\sigma} \tilde{X} - \tilde{Y}\|_F^2$, where $\tilde{Y} := Q_\sigma^\top Y$. Hence, M in $\mathcal{E}_{r,n \times n}^\sigma(\mathbb{R})$ minimizes the squared-error loss with data matrices X, Y if and only if the block diagonal matrix $B := M^{\sim Q_\sigma}$ in $(\mathcal{E}_{r,n \times n}^\sigma(\mathbb{R}))^{\sim Q_\sigma}$ minimizes the squared-error loss with data matrices \tilde{X}, \tilde{Y} . Equivalently, by Lemma 2.3, B minimizes $\|B - U\|_{\tilde{X}\tilde{X}^\top}^2$.

Step 2. *With respect to the inner product $\langle \cdot, \cdot \rangle_{\tilde{X}\tilde{X}^\top}$, compute the orthogonal projection \tilde{U} of U onto the linear space $(\mathcal{E}_{n \times n}^\sigma(\mathbb{R}))^{\sim Q_\sigma}$.*

Since $\|B - U\|_{\tilde{X}\tilde{X}^\top}^2 = \|B - \tilde{U}\|_{\tilde{X}\tilde{X}^\top}^2 + \|\tilde{U} - U\|_{\tilde{X}\tilde{X}^\top}^2$, the point on the variety $(\mathcal{E}_{r,n \times n}^\sigma(\mathbb{R}))^{\sim Q_\sigma}$ closest (w.r.t. $\|\cdot\|_{\tilde{X}\tilde{X}^\top}$) to either \tilde{U} or U is the same. The matrices in the linear space $(\mathcal{E}_{n \times n}^\sigma(\mathbb{R}))^{\sim Q_\sigma}$, including \tilde{U} , are block diagonal matrices, whose blocks are either in $\mathcal{M}_{d_i \times d_i}(\mathbb{R})$ or $\mathcal{R}(\mathcal{M}_{d_i \times d_i}(\mathbb{C}))$. Using Lemma 2.9, we can solve the $\|\cdot\|_{\tilde{X}\tilde{X}^\top}$ -distance problem from \tilde{U} on

each block separately. Since the variety $(\mathcal{E}_{r,n \times n}^\sigma(\mathbb{R}))^{\sim Q_\sigma}$ has several irreducible components, we can find its point closest to \tilde{U} by solving the minimization problem on each component individually. Hence:

Step 3. *On each irreducible component $(\mathcal{E}_{r,n \times n}^{\sigma,r}(\mathbb{R}))^{\sim Q_\sigma}$ (described in Theorem 4.8) and on each diagonal matrix block (i.e., on each factor of the direct product (4.19)), resp., solve*

$$\arg \min_{B_l \in \mathcal{M}_{r_l, m, d_l \times d_l}(\mathbb{R})} \|B_l - \tilde{U}_l\|_{\tilde{X}_l \tilde{X}_l^\top}^2 \quad \text{and} \quad \arg \min_{B_l \in \mathcal{R}(\mathcal{M}_{r_l, m, d_l \times d_l}(\mathbb{C}))} \|B_l - \tilde{U}_l\|_{\tilde{X}_l \tilde{X}_l^\top}^2, \quad (4.27)$$

respectively, using Eckart–Young (see Proposition 4.15), where \tilde{U}_l denote the blocks of \tilde{U} , and \tilde{X}_l consists of the corresponding rows of \tilde{X} .

Writing B_l^r for the solutions of these subproblems, we consider the block diagonal matrices $\bigoplus_l B_l^r$, one for each irreducible component indexed by \mathbf{r} . Out of these finitely many matrices, the one that is $\|\cdot\|_{\tilde{X} \tilde{X}^\top}$ -closest to \tilde{U} is the matrix B from Step 1. Hence, $Q_\sigma B Q_\sigma^\top$ is a σ -equivariant matrix of rank at most r that minimizes the squared-error loss with data matrices X, Y .

The only ingredient in this algorithm that is missing an explanation, is how to minimize the squared-error loss in (4.27) on spaces of realization matrices. The following lemma shows that we can reduce this problem to spaces of matrices without any special structure imposed.

Lemma 4.14. *Let $A \in \mathcal{R}(\mathcal{M}_{m \times n}(\mathbb{C}))$ and let $T \in \mathbb{R}^{n \times n}$ be a positive definite matrix. Then*

$$\|A\|_T^2 = \|A_{\text{odd}}\|_{T+PTP^\top}^2, \quad (4.28)$$

where $A_{\text{odd}} \in \mathcal{M}_{m \times 2n}(\mathbb{R})$ consists of all odd rows of A and $P := \begin{pmatrix} 0 & 1 \\ -1 & 0 \end{pmatrix} \oplus \dots \oplus \begin{pmatrix} 0 & 1 \\ -1 & 0 \end{pmatrix} \in \mathbb{R}^{2n \times 2n}$.

Proof. Let A_{even} be the $m \times 2n$ matrix that consists of all even rows of A . Since A is a realization matrix, we have that $A_{\text{even}} = A_{\text{odd}} \cdot P$. Therefore,

$$\begin{aligned} \|A\|_T^2 &= \|AT^{1/2}\|_F^2 = \|A_{\text{odd}}T^{1/2}\|_F^2 + \|A_{\text{even}}T^{1/2}\|_F^2 = \|A_{\text{odd}}T^{1/2}\|_F^2 + \|A_{\text{odd}}PT^{1/2}\|_F^2 \\ &= \text{tr}(A_{\text{odd}}TA_{\text{odd}}^\top) + \text{tr}(A_{\text{odd}}PTP^\top A_{\text{odd}}^\top) = \text{tr}(A_{\text{odd}}(T + PTP^\top)A_{\text{odd}}^\top) \\ &= \|A_{\text{odd}}\|_{T+PTP^\top}^2, \end{aligned} \quad (4.29)$$

concluding the proof. □

Proposition 4.15. *Both minimization problems in (4.27) can be solved with Eckart–Young and have SEdegree = EDdegree = $\binom{d_l}{r_l, m}$.*

Proof. We use Example 2.5 for blocks of the form $\mathcal{M}_{r_l, m, d_l \times d_l}(\mathbb{R})$. For blocks of the form $\mathcal{R}(\mathcal{M}_{r_l, m, d_l \times d_l}(\mathbb{C}))$, we consider the orthogonal projection \tilde{U}_l° from \tilde{U}_l (with respect to the inner product $\langle \cdot, \cdot \rangle_{\tilde{X} \tilde{X}^\top}$) onto the linear space $\mathcal{R}(\mathcal{M}_{d_l \times d_l}(\mathbb{C}))$. The same point on the variety $\mathcal{R}(\mathcal{M}_{r_l, m, d_l \times d_l}(\mathbb{C}))$ minimizes the $\|\cdot\|_{\tilde{X} \tilde{X}^\top}$ -distance to \tilde{U}_l and \tilde{U}_l° . Now, we delete all the even rows in the orthogonal projection \tilde{U}_l° and denote the result by $\tilde{U}_l^{\text{odd}} \in \mathcal{M}_{d_l \times 2d_l}(\mathbb{R})$.

Deleting the same rows in $B_l \in \mathcal{R}(\mathcal{M}_{r_l, m, d_l \times d_l}(\mathbb{C}))$ gives arbitrary $d_l \times 2d_l$ matrices B_l^{odd} of rank at most $r_{l, m}$. By Lemma 4.14, we have $\|B_l - \tilde{U}_l^\circ\|_{\tilde{X}\tilde{X}^\top}^2 = \|B_l^{\text{odd}} - \tilde{U}_l^{\text{odd}}\|_S^2$, where $S := \tilde{X}\tilde{X}^\top + P\tilde{X}\tilde{X}^\top P^\top$. Hence, the desired minimizer is the matrix $B_l \in \mathcal{R}(\mathcal{M}_{d_l \times d_l}(\mathbb{C}))$ such that B_l^{odd} is the matrix in $\mathcal{M}_{r_l, m, d_l \times 2d_l}(\mathbb{R})$ minimizing $\|B_l^{\text{odd}} - \tilde{U}_l^{\text{odd}}\|_S^2$. The latter can be solved with Eckart–Young (2.20) as in Example 2.5. We also see from (2.28) that both the squared-error degree and the ED degree of this problem are $\binom{d_l}{r_{l, m}}$. \square

4.3 Parameterizing equivariance and network design

One observes even in simple examples that the factors of an equivariant linear map themselves do *not* need to be equivariant.

Example 4.16. Let $\sigma = (1\ 2) \in \mathcal{S}_3$ and M be the invertible matrix

$$M = \begin{pmatrix} 1 & 2 & 0 \\ 2 & 1 & 0 \\ 3 & 3 & 4 \end{pmatrix}.$$

Indeed, $MP_\sigma = P_\sigma M$, hence M is equivariant under σ . Let $M = QR$ denote the QR decomposition of M ; uniqueness of the decomposition is obtained by imposing that R has positive diagonal entries. One can check that neither Q nor R is equivariant under σ . \diamond

Remark 4.17. The question whether the individual layers of an equivariant autoencoder are equivariant, is not well-posed in its naïve form. A priori, the group G acts only on the in- and output space of $f_\theta: \mathbb{R}^n \rightarrow \mathbb{R}^r \rightarrow \mathbb{R}^n$. To address questions about equivariance of the two individual layers, one would first need to define an action of G on \mathbb{R}^r . \diamond

In Section 3.3, we described how linear autoencoders are well-suited to parameterize permutation-invariant maps. For equivariance, auto-encoders can only parameterize the individual irreducible components of $\mathcal{E}_{r, n \times n}^\sigma$. Also in this case, the decoder and encoder inherit a weight-sharing property from the cycle decomposition of σ . To develop an intuition, we start with an example for rotation-equivariant maps of rank at most 1.

Example 4.18 (Parameterization of $\mathcal{E}_{1, 9 \times 9}^\sigma$). Let $\sigma \in \mathcal{S}_9$ again denote the rotation of a 3×3 picture by 90 degrees. Denote by P the matrix obtained by applying Step 1 of Procedure 2.16 to P_σ , i.e., P is the block diagonal matrix $\text{diag}(C_4, C_4, C_1)$. Its eigenvalues are $\{1, 1, 1, -1, -1, i, i, -i, -i\}$, here denoted as multiset together with their multiplicities. We chop M into blocks of sizes determined by the blocks of P , i.e. into blocks of size pattern

$$\left(\begin{array}{c|c|c} 4 \times 4 & 4 \times 4 & 4 \times 1 \\ \hline 4 \times 4 & 4 \times 4 & 4 \times 1 \\ \hline 1 \times 4 & 1 \times 4 & 1 \times 1 \end{array} \right).$$

Each of the blocks $M^{(i, j)}$ is circulant, as spelled out in (2.13). We are now going to describe the set of matrices M which commute with P and are of rank at most 1. For that, we will

need circulant matrices. For a vector $v = (v_1, \dots, v_n)^\top \in \mathbb{C}^n$, we denote the associated $n \times n$ circulant matrix by

$$C_n(v_1, \dots, v_n) := \begin{pmatrix} v_1 & v_2 & \cdots & v_{n-1} & v_n \\ v_n & v_1 & v_2 & \cdots & v_{n-1} \\ & & \ddots & \ddots & \\ v_3 & \cdots & v_n & v_1 & v_2 \\ v_2 & v_3 & \cdots & v_n & v_1 \end{pmatrix} \in \mathcal{M}_{n \times n}(\mathbb{C}). \quad (4.30)$$

In this notation, the circulant matrices C_n in (2.32) are $C_n = C_n(0, \dots, 0, 1)$. Imposing $r = 1$ gives rise to three irreducible components of $\mathcal{E}_{1,9 \times 9}^\sigma(\mathbb{C})$ of dimension 3, and one of dimension 5, according to Theorem 4.2. By $\mathbb{1}$, we will denote the all-one matrix; its size is determined implicitly by the rest of the matrix. An explicit analysis reveals that the general matrices in the four components of $\mathcal{E}_{1,9 \times 9}^\sigma(\mathbb{C})$ take the following forms for scalars $\alpha_1, \alpha_2, \alpha_3, \beta_1, \beta_2, \beta_3 \in \mathbb{C}$:

$$\begin{aligned} & \left(\begin{array}{c|c|c} \alpha_1\beta_1 C_4(1, 1, 1, 1) & \alpha_1\beta_2 C_4(1, 1, 1, 1) & \alpha_1\beta_3 \cdot \mathbb{1} \\ \alpha_2\beta_1 C_4(1, 1, 1, 1) & \alpha_2\beta_2 C_4(1, 1, 1, 1) & \alpha_2\beta_3 \cdot \mathbb{1} \\ \hline \alpha_3\beta_1 \cdot \mathbb{1} & \alpha_3\beta_2 \cdot \mathbb{1} & \alpha_3\beta_3 \end{array} \right), \\ & \left(\begin{array}{c|c|c} \alpha_1\beta_1 C_4(1, -1, 1, -1) & \alpha_1\beta_2 C_4(1, -1, 1, -1) & 0 \\ \alpha_2\beta_1 C_4(1, -1, 1, -1) & \alpha_2\beta_2 C_4(1, -1, 1, -1) & 0 \\ \hline 0 & 0 & 0 \end{array} \right), \\ & \left(\begin{array}{c|c|c} \alpha_1\beta_1 C_4(1, -i, -1, i) & \alpha_1\beta_2 C_4(1, -i, -1, i) & 0 \\ \alpha_2\beta_1 C_4(1, -i, -1, i) & \alpha_2\beta_2 C_4(1, -i, -1, i) & 0 \\ \hline 0 & 0 & 0 \end{array} \right), \\ & \left(\begin{array}{c|c|c} \alpha_1\beta_1 C_4(1, i, -1, -i) & \alpha_1\beta_2 C_4(1, i, -1, -i) & 0 \\ \alpha_2\beta_1 C_4(1, i, -1, -i) & \alpha_2\beta_2 C_4(1, i, -1, -i) & 0 \\ \hline 0 & 0 & 0 \end{array} \right). \end{aligned} \quad (4.31)$$

The first component is isomorphic to the affine cone over the Segre variety $\mathbb{P}_{\mathbb{C}}^2 \times \mathbb{P}_{\mathbb{C}}^2$, the remaining three are isomorphic to the affine cone over the Segre variety $\mathbb{P}_{\mathbb{C}}^1 \times \mathbb{P}_{\mathbb{C}}^1$ each. Only the first two of them appear in the real locus $\mathcal{E}_{1,9 \times 9}^\sigma(\mathbb{R})$; cf. Theorem 4.8. The matrices in those two components can be factorized as follows:

$$\begin{aligned} & (\alpha_1, \alpha_1, \alpha_1, \alpha_1, \alpha_2, \alpha_2, \alpha_2, \alpha_2, \alpha_3)^\top \cdot (\beta_1, \beta_1, \beta_1, \beta_1, \beta_2, \beta_2, \beta_2, \beta_2, \beta_3), \\ & (\alpha_1, -\alpha_1, \alpha_1, -\alpha_1, \alpha_2, -\alpha_2, \alpha_2, -\alpha_2, 0)^\top \cdot (\beta_1, -\beta_1, \beta_1, -\beta_1, \beta_2, -\beta_2, \beta_2, -\beta_2, 0). \end{aligned} \quad (4.32)$$

These factorizations are linear autoencoders $\mathbb{R}^9 \rightarrow \mathbb{R}^1 \rightarrow \mathbb{R}^9$ with the same weight-sharing on the en- and decoder. \diamond

In Section 4.1.2, we characterized the real irreducible components in general. We here present a parameterization for each of the irreducible components described in Theorem 4.8. For that, we consider the following parameterization of $\mathcal{M}_{r,n \times n}(\mathbb{C})$:

$$\mu_{r,n}^{\mathbb{C}}: \mathcal{M}_{n \times r}(\mathbb{C}) \times \mathcal{M}_{r \times n}(\mathbb{C}) \longrightarrow \mathcal{M}_{r,n \times n}(\mathbb{C}), \quad (A, B) \mapsto A \cdot B. \quad (4.33)$$

Hence, we will write every element of $\mathcal{M}_{r,n \times n}(\mathbb{C})$ as a product of two matrices A and B ; they will play the role of a decoder and encoder, respectively. Since \mathcal{R} is an isomorphism of rings, the complex matrix-multiplication map extends to realization spaces:

$$\begin{aligned} \mathcal{R}\mu_{r,n}^{\mathbb{C}}: \mathcal{R}(\mathcal{M}_{n \times r}(\mathbb{C})) \times \mathcal{R}(\mathcal{M}_{r \times n}(\mathbb{C})) &\rightarrow \mathcal{R}(\mathcal{M}_{r,n \times n}(\mathbb{C})), \\ (\mathcal{R}(A), \mathcal{R}(B)) &\mapsto \mathcal{R}(A) \cdot \mathcal{R}(B) = \mathcal{R}(A \cdot B). \end{aligned} \quad (4.34)$$

Proposition 4.19. *Let $\mu_{r_1,1,d_1}$ and $\mu_{r_2,1,d_2}$ denote the real parameterization maps from Lemma 3.10 for $\mathcal{M}_{r_1,1,d_1 \times d_1}(\mathbb{R})$ and $\mathcal{M}_{r_2,1,d_2 \times d_2}(\mathbb{R})$, respectively. Let $\mu_{r_l,m,d_l}^{\mathbb{C}}$ be the complex parameterization of $\mathcal{M}_{r_l,m,d_l \times d_l}(\mathbb{C})$, for $l \geq 3$. Then the real irreducible component of $(\mathcal{E}_{r,n \times n}^{\sigma})^{\sim Q_{\sigma}}$ corresponding to $\mathbf{r} = (r_{l,m})$ as in Theorem 4.8 is parameterized by the map*

$$\mu_{\mathbf{r},n} := \mu_{r_1,1,d_1} \times \mu_{r_2,1,d_2} \times \prod_{l \geq 3} \prod_{\substack{m \in (\mathbb{Z}/l\mathbb{Z})^{\times}, \\ \frac{1}{2} < \frac{m}{l} < 1}} \mathcal{R}\mu_{r_l,m,d_l}^{\mathbb{C}}, \quad (4.35)$$

where Q_{σ} is the realization base change of P_{σ} .

Proof. After the base change Q_{σ} , every matrix in the real irreducible component corresponding to the integer solution \mathbf{r} has the block diagonal structure (4.19). The blocks associated with $l \geq 3$ and $\frac{1}{2} < \frac{m}{l} < 1$ are the realization of $\mathcal{M}_{r_l,m,d_l \times d_l}(\mathbb{C})$, so they admit a parameterization via $\mathcal{R}\mu_{r_l,m,d_l}^{\mathbb{C}}$. Therefore, the real component $(\mathcal{E}_{r,n \times n}^{\sigma,\mathbf{r}})^{\sim Q_{\sigma}}$ is parameterized by $\mu_{\mathbf{r},n}$. \square

As a direct consequence of the parameterization in (4.35), one deduces a sparsity of the encoder and decoder into which the matrices of the respective irreducible component decompose into. We also obtain a weight-sharing property arising from the realization matrix blocks: the entries on the diagonal of each such matrix are equal, and the ones on the anti-diagonal differ only by a sign. We now demonstrate these findings in our running example of rotation-invariance.

Example 4.20. We revisit Example 4.9. The real irreducible component $(\mathcal{E}_{3,9 \times 9}^{\sigma,\mathbf{r}})^{\sim Q_{\sigma}}$ with $\mathbf{r} = (1, 0, 1)$ is

$$\mathcal{M}_{1,3 \times 3}(\mathbb{R}) \times \mathcal{M}_{0,2 \times 2}(\mathbb{R}) \times \mathcal{R}(\mathcal{M}_{1,2 \times 2}(\mathbb{C})). \quad (4.36)$$

By Proposition 4.19, this component is parameterized by $\mu_{\mathbf{r},3} = \mu_{1,3} \times \mu_{0,2} \times \mathcal{R}\mu_{1,2}^{\mathbb{C}}$. Thus, every matrix in (4.36) can be obtained as product of a 9×3 and a 3×9 matrix of the form

$$\begin{pmatrix} * & * & * & 0 & 0 & 0 & 0 & 0 & 0 \\ 0 & 0 & 0 & 0 & 0 & & & & \\ 0 & 0 & 0 & 0 & 0 & \mathcal{R}(\star & \star) & & \end{pmatrix}^{\top} \cdot \begin{pmatrix} * & * & * & 0 & 0 & 0 & 0 & 0 & 0 \\ 0 & 0 & 0 & 0 & 0 & & & & \\ 0 & 0 & 0 & 0 & 0 & \mathcal{R}(\star & \star) & & \end{pmatrix}, \quad (4.37)$$

where $*$ and \star represent arbitrary real and complex entries, respectively. The induced weight-sharing property on the encoder and decoder is visualized in Figure 3. \diamond

A parameterization of $\mathcal{E}_{r,n \times n}^{\sigma,\mathbf{r}}$ is obtained by simply composing the autoencoders described in this section with the fixed matrix Q_{σ} on the left, and its inverse Q_{σ}^{\top} on the right. However, the sparsity of the weights of the en- and decoder is easiest observed via the block diagonal form (4.19). For this reason, we formulated Proposition 4.19 for $(\mathcal{E}_{r,n \times n}^{\sigma,\mathbf{r}})^{\sim Q_{\sigma}}$.

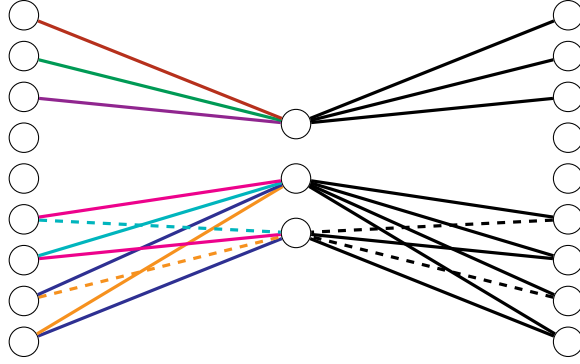


Figure 3: Weight-sharing of the encoder and decoder matrices from Example 4.20. Edges of the same color share the same weight—and differ by sign, in case one of the edges is dashed. To avoid an overload of colors, we here visualized the weight-sharing for the encoder only; the decoder follows the same rules, but would require additional seven color shades. Due to the zero blocks in (4.37), the 4th and 5th input and output neurons are inactive.

4.4 Induced filtration of $\mathcal{M}_{r,n \times n}$

Let $\sigma \in \mathcal{S}_n$. Whenever a matrix is equivariant under σ , then it is also equivariant under any power of σ . Hence, $\mathcal{E}_{n \times n}^{\sigma^k} \subset \mathcal{E}_{n \times n}^{\sigma^{l+k}}$ for all $k, l \in \mathbb{N}$. Therefore, any $\sigma \in \mathcal{S}_n$ gives rise to an increasing filtration $\mathcal{E}_{n \times n}^{\sigma^\bullet}$ of \mathcal{M} . This filtration is finite: every permutation has a finite order, hence $\mathcal{E}^{\sigma^l} = \mathcal{E}_{n \times n}^{\text{id}} = \mathcal{M}_{n \times n}$ for $l = \text{ord}(\sigma)$. By intersecting with $\mathcal{M}_{r,n \times n}$, we obtain analogous statements for $\mathcal{E}_{r,n \times n}^{\sigma^\bullet}$.

4.5 Example: Equivariance for non-cyclic groups

We here revisit equivariance for 3×3 pictures. Characterizing equivariance for non-cyclic permutation groups is more complicated than the cyclic case. As a case study, we impose equivariance both under rotation and under reflection, i.e., we consider the group $G = \langle \sigma, \chi \rangle$ generated by the clock-wise rotation by 90 degrees σ as in (2.1), and the reflection

$$\chi: \begin{pmatrix} a_{11} & a_{12} & a_{13} \\ a_{21} & a_{22} & a_{23} \\ a_{31} & a_{32} & a_{33} \end{pmatrix} \mapsto \begin{pmatrix} a_{13} & a_{12} & a_{11} \\ a_{23} & a_{22} & a_{21} \\ a_{33} & a_{32} & a_{31} \end{pmatrix}. \quad (4.38)$$

We will again identify $\mathbb{R}^{3 \times 3} \cong \mathbb{R}^9$ via

$$\begin{pmatrix} a_{11} & a_{12} & a_{13} \\ a_{21} & a_{22} & a_{23} \\ a_{31} & a_{32} & a_{33} \end{pmatrix} \mapsto (a_{11} \ a_{13} \ a_{33} \ a_{31} \ a_{12} \ a_{23} \ a_{32} \ a_{21} \ a_{22})^\top. \quad (4.39)$$

Then $\chi(A)$ is represented by the vector $(a_{13} \ a_{11} \ a_{31} \ a_{33} \ a_{12} \ a_{21} \ a_{32} \ a_{23} \ a_{22})^\top$. Under this identification, the reflection is $\chi = (12)(34)(68) \in \mathcal{S}_9$, and we denote its representing matrix by P_χ . Hence, equivariance of a matrix $M = (m_{ij})_{i,j} \in \mathcal{M}_{9 \times 9}$ under both σ and χ ,

i.e., $MP_\sigma = P_\sigma M$ and $MP_\chi = P_\chi M$, implies that M has to be of the form

$$M = \left(\begin{array}{c|c|c} C_4(\alpha_1, \alpha_2, \alpha_3, \alpha_2) & C_4(\beta_1, \beta_2, \beta_2, \beta_1) & \varepsilon_3 \cdot \mathbb{1} \\ \hline C_4(\gamma_1, \gamma_1, \gamma_3, \gamma_3) & C_4(\delta_1, \delta_2, \delta_3, \delta_2) & \varepsilon_4 \cdot \mathbb{1} \\ \hline \varepsilon_1 \cdot \mathbb{1} & \varepsilon_2 \cdot \mathbb{1} & \varepsilon_5 \end{array} \right). \quad (4.40)$$

Therefore, $\dim(\mathcal{E}_{9 \times 9}^G) = 81 - 66 = 2 \cdot 3 + 2 \cdot 2 + 5 \cdot 1 = 15$. In comparison to matrices that are required to be equivariant under the rotation σ only (see (2.13)), the entries $\alpha_4, \beta_3, \beta_4, \gamma_2, \gamma_4$, and δ_4 can no longer be chosen freely, which drops the dimension by 6.

Let us add the action of another permutation on 3×3 pictures, namely shifting each row by one to the right, i.e., for $i = 1, 2, 3$, $a_{i,j} \mapsto a_{i,j+1}$ for $j = 1, 2$, and $a_{i,3} \mapsto a_{i,1}$. In the choice from above, the shift corresponds to the permutation $(1\ 5\ 2)(3\ 4\ 7)(6\ 8\ 9) \in \mathcal{S}_9$. All 9×9 matrices M that are equivariant under rotation, reflection, and shift, are of the following form, with only 3 degrees $\alpha_1, \alpha_2, \alpha_3$ of freedom:

$$M = \left(\begin{array}{c|c|c} C_4(\alpha_1, \alpha_2, \alpha_3, \alpha_2) & C_4(\alpha_2, \alpha_3, \alpha_3, \alpha_2) & \alpha_3 \cdot \mathbb{1} \\ \hline C_4(\alpha_2, \alpha_2, \alpha_3, \alpha_3) & C_4(\alpha_1, \alpha_3, \alpha_2, \alpha_3) & \alpha_2 \cdot \mathbb{1} \\ \hline \alpha_3 \cdot \mathbb{1} & \alpha_2 \cdot \mathbb{1} & \alpha_1 \end{array} \right). \quad (4.41)$$

To understand the general behavior, one will need to engage in combinatorial tailoring.

5 Experiments

We apply our findings to train various linear autoencoders on the dataset MNIST [5], a widely used benchmark in machine learning. Our implementations in Python [18] are made available at <https://github.com/vahidshahverdi/Equivariant>. MNIST comprises 60,000 training and 10,000 test black-and-white images of handwritten digits, each with a size of 28×28 pixels. Utilizing MNIST images, we introduce random horizontal shifts of up to six pixels. Some representative images from the test dataset are shown in Figure 4. The task at hand is to design an autoencoder that is equivariant under horizontal translations. To achieve this, we first consider the permutation $\sigma \in \mathcal{S}_{784}$, representing a horizontal shift by one pixel. Consequently, we have 28 disjoint cycles of size 28, one for each row of images. The input data matrix X is a real matrix of size $784 \times 60,000$, where each column of X represents the row-wise vectorization of the shifted images. It is important to note that, due to the structure of images, X does not yield a full-rank matrix; in fact, its rank is $397 < 784$. We choose $r = 99$, and our goal is to find a matrix $M^{\sim Q_\sigma} = \bigoplus_{i=0}^{14} M_i$ in $(\mathcal{E}_{99,784 \times 784}^\sigma)^{\sim Q_\sigma}$ such that M minimizes $\|MX - X\|_F^2$. In here, M_0 and M_{14} are matrices in $\mathcal{M}_{r_0, 28 \times 28}$ and $\mathcal{M}_{r_{14}, 28 \times 28}$, respectively, and $M_i \in \mathcal{R}(\mathcal{M}_{r_i, 28 \times 28}(\mathbb{C}))$ for $i = 1, \dots, 13$, where $r_0 + 2r_1 + \dots + 2r_{13} + r_{14} = 99$. For increased readability, we write r_i instead of $r_{l,m}$; see Equation (5.2) for the precise matching of the indices. As explained in Section 4.3, any network can parameterize only one of the real irreducible components $\mathcal{E}_{r,784 \times 784}^{\sigma,r}$ of $\mathcal{E}_{r,784 \times 784}^\sigma$. Referring to Theorem 4.2, we find that the number of irreducible components of $\mathcal{E}_{r,784 \times 784}^\sigma$ is

$$72,425,986,088,826. \quad (5.1)$$



Figure 4: *Top row*: Nine samples from the MNIST [5] test dataset, shifted horizontally randomly by up to six pixels. *Middle row*: Output of a linear equivariant autoencoder designed to be equivariant under horizontal translations. The network architecture is determined by the integer vector \mathbf{r} , as described in Equation (5.2). *Bottom row*: Output of a dense linear autoencoder with bottleneck $r = 99$ and no equivariance imposed.

Among these numerous components, we empirically observed that the component corresponding to the following integer vector \mathbf{r} yields a reasonable loss for $r = 99$:

$$\begin{aligned}
 \mathbf{r} &= (r_0, r_1, r_2, r_3, r_4, r_5, r_6, r_7, r_8, r_9, r_{10}, r_{11}, r_{12}, r_{13}, r_{14}) \\
 &= (r_{1,1}, r_{28,27}, r_{14,13}, r_{28,25}, r_{7,6}, r_{28,23}, r_{14,11}, r_{4,3}, r_{7,5}, r_{28,19}, r_{14,9}, r_{28,17}, r_{7,4}, r_{28,15}, r_{2,1}) \quad (5.2) \\
 &= (13, 10, 9, 8, 7, 5, 3, 1, 0, 0, 0, 0, 0, 0, 0).
 \end{aligned}$$

The choice of the $r_{l,m}$ depends entirely on the structure of the data. Our observation reveals that, in each column of X , the energy is concentrated in low frequencies, as is illustrated in Figure 6. Consequently, the blocks corresponding to eigenvalues $\lambda_{l,m} = e^{\frac{2\pi m}{l}}$ with phases close to the zero angle contain more information. Thus, to effectively encode this information, it might be required to put higher ranks on blocks M_i for i close to 0. Figure 5 is a visual representation of this energy distribution for each Fourier mode. In Figure 4, we showcase the output for nine samples using our equivariant autoencoder with architecture \mathbf{r} , and compare it to a linear autoencoder with $r = 99$, without equivariance imposed.

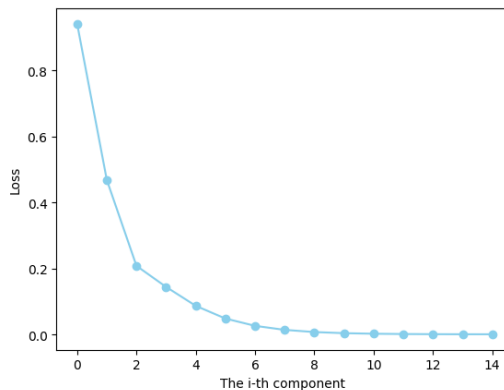


Figure 5: The error incurred by the block M_i , $i = 0, \dots, 14$, when setting $\text{rank}(M_i) = 0$.

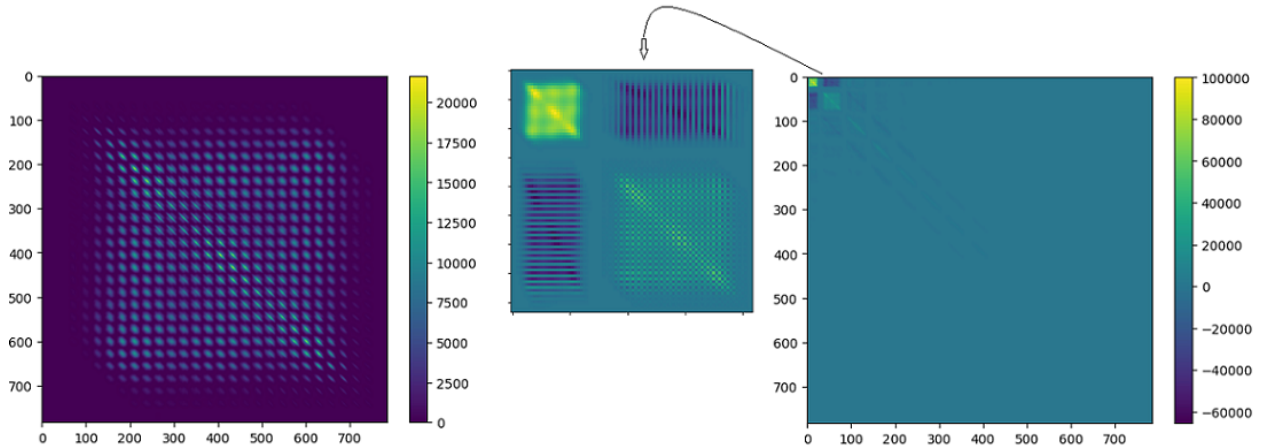


Figure 6: On the left, XX^\top is visualized as an image, where X represents our input data. On the right, $(XX^\top)^{\sim Q_\sigma}$ is depicted, with Q_σ as defined in Section 4.1.2. Analyzing the plot on the right hand side, we note that the majority of the signal’s energy is concentrated in low frequencies.

The significance of a proper choice of \mathbf{r} is illustrated in Figure 7. In this figure, we present the outputs of a handwritten digit “6” under two different equivariant architectures: first, using $r_{l,m} = 7$ for every l and m , and second, by excluding the first seven blocks following the order in (5.2), and the remaining blocks having full rank. Despite both scenarios having a total rank r greater than 99, the outcomes are notably inferior.

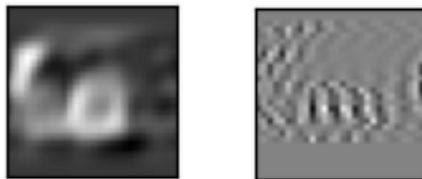


Figure 7: The outputs of linear equivariant autoencoders with suboptimal architectures for a handwritten digit “6”. *On the left:* an equivariant autoencoder with equal rank distributed among the blocks, setting all $r_{l,m} = 7$. *On the right:* High-pass equivariant autoencoder, excluding the first seven blocks in the order of (5.2).

From the comparison presented in Table 1, one reads that a dense linear autoencoder without imposed equivariance—on average—outperforms equivariant architectures in terms of the mean squared loss. However, achieving this superior performance demands a substantial parameter count, totaling $2 \cdot 99 \cdot 784 = 155,232$. In contrast, our proposed equivariant autoencoder, defined by the architecture in (5.2), requires a more efficient parameter count of $2 \cdot (28 \cdot 13 + 2 \cdot 28 \cdot (10 + 9 + 8 + 7 + 5 + 3 + 1)) = 5,544$. It is worth mentioning that, since we empirically chose one of the numerous irreducible components of $\mathcal{E}_{99,784 \times 784}^\sigma$, our

proposed equivariant autoencoder may not represent the optimal choice among all possible linear equivariant architectures with $r = 99$.

	Equivariant architecture (5.2)	equal-rank equivariant	high-pass equivariant	non-equivariant
Loss	0.0082	0.0206	0.1063	0.0057

Table 1: Comparison of average square loss values per pixel between linear equivariant and non-equivariant autoencoders on the MNIST test dataset. The equal-rank equivariant architecture is achieved by setting all $r_{l,m} = 7$, while the high-pass equivariant architecture is obtained by letting the first seven blocks have rank 0, and the remaining blocks have full rank. The non-equivariant network is trained with $r = 99$.

The non-equivariant linear autoencoder with a bottleneck size of $r = 99$ exhibits partial equivariance under horizontal shifts, as depicted in Figure 8. This behavior arises from the fact that for larger shifts, handwritten digits could split into two parts (scenarios which are not—or only barely—present in our modified dataset). This observation might be a partial explanation for the superior performance of the dense linear autoencoder compared to our equivariant architecture—the latter, however, is more efficient.

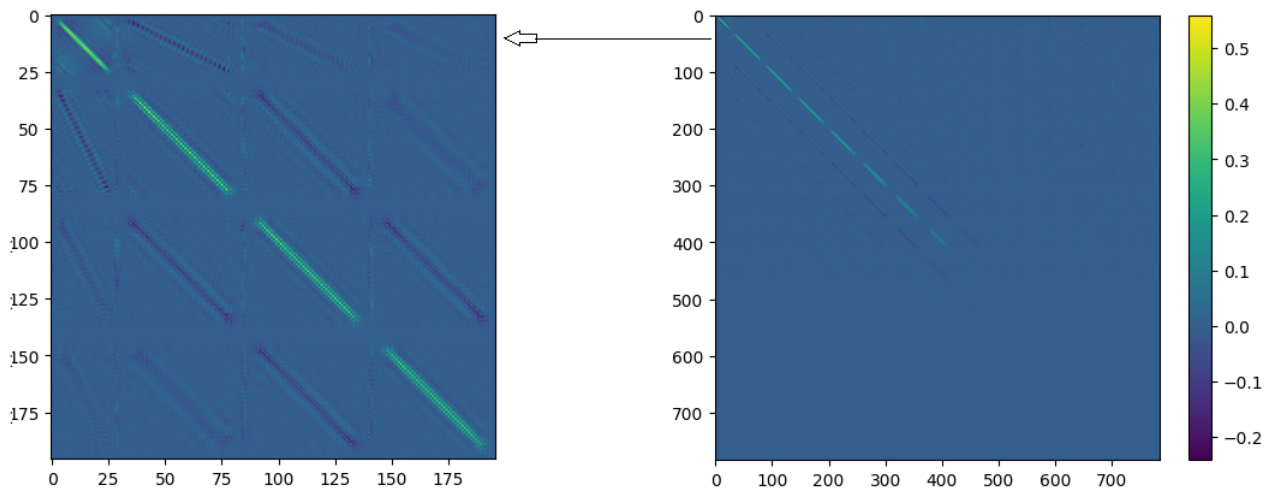


Figure 8: The plot on the right represents the trained dense linear autoencoder with bottleneck $r = 99$ after the base change by $Q^{\sim\sigma}$. The one on the left is a magnified image of the plot on the right. It is evident that this final matrix is only partially equivariant under horizontal translations.

6 Conclusion and outlook

We investigated linear neural networks through the lens of algebraic geometry, with an emphasis on linear autoencoders. Their function spaces are determinantal varieties $\mathcal{M}_{r,n \times n}$ in a natural way. We considered permutation groups G and fully characterized the elements of the function space which are invariant under the action of G . They form an irreducible algebraic variety $\mathcal{I}_{r,n \times n}^G \subset \mathcal{M}_{r,n \times n}$ for which we computed the dimension, singular points, and degree. We showed that the squared-error loss can be minimized on that variety by an explicit calculation using the Eckart–Young theorem. We proved that all G -invariant functions can be parameterized by a linear autoencoder, and we derived implications for the design of such an autoencoder, namely a dimensional constraint on the middle layer and weight sharing in the encoder. For equivariance, we treated cyclic subgroups $G = \langle \sigma \rangle$ of permutation groups. Also in this case, the resulting part of the function space is an algebraic variety $\mathcal{E}_{r,n \times n}^\sigma \subset \mathcal{M}_{r,n \times n}$. Typically, this variety has several irreducible components; we determined them both over \mathbb{C} and over \mathbb{R} . We computed their dimension, singular locus, and degree (the latter only for the complex components). Since $\mathcal{E}_{r,n \times n}^\sigma$ is reducible, no linear neural network can parameterize all of $\mathcal{E}_{r,n \times n}^\sigma$. However, we provided a parameterization of each real irreducible component via a sparse autoencoder with the same weight sharing on its en- and decoder. We also explained a simple algorithm that reduces squared-error loss minimization on each real component to applying the Eckart–Young theorem multiple times.

To showcase our results, we trained several autoencoders on the MNIST dataset. For a bottleneck rank of $r = 99$, the space of linear functions that are equivariant under horizontal shifts has the gigantic number 72,425,986,088,826 of real irreducible components. We carefully chose one of the components and compared the outcome of an equivariant autoencoder parametrizing that component with a linear autoencoder without imposed equivariance. The latter did achieve a lower loss, requires however significantly more parameters. We also give a partial explanation of the superior performance of a general linear network; it arises from the nature of the considered dataset, which might be partially equivariant only.

The generalization to non-cyclic groups is more intricate than for invariance. We plan to tackle this problem in follow-up work. One should also address groups other than permutation groups, such as non-discrete groups. Another natural step to take is to generalize the network architecture to a bigger number of layers as well as to allowing non-trivial activation functions, such as ReLU. For the latter, we expect that tropical expertise will be helpful to study the resulting geometry of the function space. Having the geometry of the function spaces understood, one should also investigate the types of critical points during training processes and how they compare to networks without imposed equi- or invariance.

Acknowledgments.

We thank Joakim Andén and Luca Sodomaco for insightful discussions on our experiments and on ED degrees, respectively. KK and ALS were partially supported by the Wallenberg AI, Autonomous Systems and Software Program (WASP) funded by the Knut and Alice Wallenberg Foundation.

References

- [1] E. J. Bekkers, M. Lafarge, M. Veta, K. Eppenhof, J. Pluim, and R. Duits. Roto-translation covariant convolutional networks for medical image analysis. In *Medical Image Computing and Computer Assisted Intervention – MICCAI 2018 - 21st International Conference, 2018, Proceedings*, Lecture Notes in Computer Science, pages 440–448. Springer, 2018. 4
- [2] E. J. Bekkers. B-spline CNNs on Lie groups. In *8th International Conference on Learning Representations, ICLR 2020, Addis Ababa, 30 April 2020*, 2020. 4
- [3] P. Breiding, K. Kohn, and B. Sturmfels. *Metric Algebraic Geometry*. Oberwolfach Seminars. Birkhäuser, Basel, 2024. Open access, available at https://kathlenkohn.github.io/Papers/MFO_Seminar_MAG.pdf. 10
- [4] T. S. Cohen and M. Welling. Group equivariant convolutional networks. In *Proceedings of the 33rd International Conference on Machine Learning*, volume 48 of *Proceedings of Machine Learning Research*, pages 2990–2999. PMLR, 2016. 4
- [5] L. Deng. The MNIST Database of Handwritten Digit Images for Machine Learning Research. *IEEE Signal Pro. Mag.*, 29(6):141–142, 2012. 35, 36
- [6] P. Dhar. The carbon impact of artificial intelligence. *Nat. Mach. Intell.*, 2:423–425, 2020. 2
- [7] S. Di Rocco, L. Gustafsson, and L. Sodomaco. Conditional Euclidean distance optimization via relative tangency. Preprint arXiv:2310.16766, 2023.
- [8] J. Draisma, E. Horobet, G. Ottaviani, B. Sturmfels, and R. R. Thomas. The Euclidean Distance Degree of an Algebraic Variety. *Found. Comput. Math.*, 16:99–149, 2016. 10, 12
- [9] W. Fulton. *Intersection Theory*. Springer-Verlag, 1984. 11
- [10] D. R. Grayson and M. E. Stillman. Macaulay2, a software system for research in algebraic geometry. Available at <http://www.math.uiuc.edu/Macaulay2/>. 10
- [11] J. Harris. *Algebraic Geometry. A First Course*, volume 133 of *Graduate Texts in Mathematics*. Springer, 1992. 11
- [12] K. Kohn, T. Merkh, G. Montufár, and M. Trager. Geometry of Linear Convolutional Networks. *SIAM J. Appl. Algebra Geom.*, 6, 2022. 3
- [13] K. Kohn, G. Montufár, V. Shahverdi, and M. Trager. Function Space and Critical Points of Linear Convolutional Networks. Preprint arXiv:2304.05752, 2023. 3
- [14] L.-H. Lim and B. J. Nelson. What is an equivariant neural network? *Notices Amer. Math. Soc.*, 70(4):619–625, 2023. 4
- [15] G. M. Nguegnang, H. Rauhut, and U. Terstiege. Convergence of gradient descent for learning linear neural networks. Preprint arXiv:2108.02040, 2021. 3
- [16] R. Schwartz, J. Dodge, N. A. Smith, and O. Etzioni. Green AI. *Commun. ACM*, 63(12):54–63, 2020. 2
- [17] M. Trager, K. Kohn, and J. Bruna. Pure and spurious critical points: a geometric study of linear networks. In *8th International Conference on Learning Representations, ICLR 2020, Addis Ababa, 30 April 2020*, 2020. 3, 19
- [18] G. Van Rossum and F. L. Drake. *Python 3 Reference Manual*. CreateSpace, Scotts Valley, CA, 2009. 35
- [19] M. Weiler, P. Forré, E. Verlinde, and M. Welling. Coordinate independent convolutional networks – isometry and gauge equivariant convolutions on Riemannian manifolds. Preprint arXiv:2106.06020, 2021. 4
- [20] J. Wood and J. Shawe-Taylor. A unifying framework for invariant pattern recognition. *Pattern Recognit. Lett.*, 17(14):1415–1422, 1996. 4